Computers and Concrete, *Vol. 23, No. 5 (2019) 361-376*
DOI: https://doi.org/10.12989/cac.2019.23.5.361

Bending analysis of a micro sandwich skew plate using extended Kantorovich method based on Eshelby-Mori-Tanaka approach

Javad Rajabi and Mehdi Mohammadimehr*

Department of Solid Mechanics, Faculty of Mechanical Engineering, University of Kashan, P.O. Box: 87317-53153, Kashan, Iran

(Received March 3, 2019, Revised April 13, 2019, Accepted April 19, 2019)

Abstract. In this research, bending analysis of a micro sandwich skew plate with isotropic core and piezoelectric composite face sheets reinforced by carbon nanotube on the elastic foundations are studied. The classical plate theory (CPT) are used to model micro sandwich skew plate and to apply size dependent effects based on modified strain gradient theory. Eshelby-Mori-Tanaka approach is considered for the effective mechanical properties of the nanocomposite face sheets. The governing equations of equilibrium are derived using minimum principle of total potential energy and then solved by extended Kantorovich method (EKM). The effects of width to thickness ratio and length to width of the sandwich plate, core-to-face sheet thickness ratio, the material length scale parameters, volume fraction of CNT, the angle of skew plate, different boundary conditions and types of cores on the deflection of micro sandwich skew plate are investigated. One of the most important results is the reduction of the deflection by increasing the angle of the micro sandwich skew plate and decreasing the deflection by decreasing the thickness of the structural core. The results of this research can be used in modern construction in the form of reinforced slabs or stiffened plates and also used in construction of bridges, the wing of airplane.

Keywords: bending analysis; micro sandwich skew plate; piezoelectric composite face sheets; extended Kantorovich method, Eshelby-Mori-Tanaka approach

1. Introduction

The skew plates find wide range of application in civil, aerospace, naval, mechanical engineering structures. They are mostly used particularly in civil and mechanical engineering fields in construction of bridges, the wing of airplane, body of ships, tails and fins of aircrafts, and parallelogram slabs in buildings. However, several alternatives are also available for analyzing such complex problems by approximate methods including finite element methods, differential quadrature method (DQM) and extended Kantorovich method (EKM).

Extended Kantorovich method is known as a method of semi-analytical solution in mechanical problems, which transforms partial differential equations into two or more ordinary differential equations (depending on the number of variables in the equations). Unlike other methods such as the Galerkin weighted residual method, the initial guess is to start the desired and even need not satisfy the boundary conditions in extended Kantorovich method. This method was first used by Kantorovich and Krylor (1960) for the numerical solution of bending problems of thin rectangular sheets in 1933. The Kantorovich method was used by Kerr (1968) to solve the torsional problem of the rectangular cross-sectional prism rod. Subsequently, this method was considered free vibration (Jones and Milne 1976), buckling (Yuan and Jin 1998, Jana and Bhaskar 2006) and strain analysis by Kim *et al.* (2000) for solving special-value problems in 1969. Extended Kantorovich method for the first time in non-Cartesian coordinates in polar coordinates was investigated by Aghdam *et al.* (2007) for analyzing the sector plate and bending analysis of the orthotropic thin plate by Aghdam and Mohammadi (2009) and for the composite cylindrical panel by Abuhamza *et al.* (2007) was investigated.

In recent decades, the smart materials are employed in nano and micro electro-mechanical or magneto-electro-elastic systems. For highly durability and enhancement of them, the smart materials such as polymeric piezoelectric nanocomposite can be reinforced by single-walled or multi-walled carbon nanotubes. Employing carbon nanotubes in these materials result in wonderful properties including transparency, electrically and thermal conductive, light weight, tolerance of different magneto-electrostatic fields. Also these materials have been used in various applications particularly in wireless strain sensor, biosensors, nanogenerator, and harvesting devises (Calleja *et al.* 2012, Yun *et al.* 2014, Arani *et al.* (2012), Mohammadimehr and Rahmati (2013), Mohammadimehr *et al.* 2016, 2017a, 2018a).

Along with the advancement of technology, materials with good quality such as lightweight, and high strength to weight ratio which is defined as the sandwich panel is produced. Tolerance and the capacity of these panels depends on the foam core and facesheet. Sandwich structures are usually composed of two thin and high strength face sheets separated by a thick and low density core layer. One of the main advantages of the sandwich panel is lightweight, and high strength to weight ratio.

*Corresponding author, Ph.D.
E-mail: mmohammadimehr@kashanu.ac.ir

ISSN: 1598-8198 (Print), 1598-818X (Online)

Based on what was said, a sandwich structure the combination of two facesheet solid and thin a lightweight core and a glue film that is bounded on two sides by two layers and in the middle of an insulating layer, this insulating material should be very soft and lightweight and has certain physical properties. Piezoelectric materials have different applications in electro-mechanical systems as sensor and actuator. These materials can be used to detect deformations and stresses or actuate a system. The piezoelectric materials can exchange input electric potential to mechanical deformation in actuating.

Calculation of displacement or electric potential in an electro-mechanical system is one of important problem of mechanical engineers. Considering the piezoelectric materials in nano scale reflects interesting behaviours that attract researchers.

In this article, some researches and applicability of sandwich structures are illustrated as follows:

Free vibration analysis of functionally graded conical, cylindrical shell and annular plate structures with a four-parameter power-law distribution is studied by Tornabene (2009). In the other work, functionally graded material (FGM) and laminated doubly curved shells and panels of revolution with a free-form meridian is performed by Tornabene *et al.* (2011). Ghorbanpour Arani *et al*. (2011a) considered thermal buckling analysis of double-walled carbon nanotubes considering the small-scale length effect. Also, in the other work, they (2011b) presented the dynamic stability of the double-walled carbon nanotube under axial loading embedded in an elastic medium by the energy method. Stress and strain recovery for functionally graded free-form and doubly-curved sandwich shells using higher-order equivalent single layer theory is considered by Tornabene *et al*. (2015). Effect of agglomeration on the natural frequencies of functionally graded carbon nanotube-reinforced laminated composite doubly-curved shells is illustrated by Tornabene *et al.* (2015). Free vibration analysis of sandwich plate with a transversely flexible core and FG-CNTs reinforced nanocomposite face sheets subjected to magnetic field and temperature-dependent material properties using SGT is studied by Mohammadimehr and Mostafavifar (2016). Moreover, Mohammadimehr and Mehrabi (2017) studied the stability and free vibration analyses of double-bonded micro composite sandwich cylindrical shells conveying fluid flow. Static analysis of functionally graded nanocomposite sandwich plates reinforced by defected CNT is studied by Moradi and Aghadavoudi (2018). It is observed that when CNT volume fraction is 5%, six vacancy defects in CNT configuration can increase the deflection of the sandwich plate up to 41.67%. Three dimensional transient analysis of FGM rectangular sandwich late subjected to thermal loading is performed by Alibeigloo and Tahri (2018). Rectangular sandwich plates with Miura-ori folded core under quasi-static loadings studied by Xiang *et al.* (2018). It has been found that the maximum bending strength is governed by the incipience or fully plastic yielding of the core material for relatively thick cores, or elastic buckling of the core compression for thin cores. Rectangular and skew shear buckling of FG-CNT reinforced composite skew plates using Ritz method is performed by Kiani and Mirzaei (2018) is verified that, the buckling load of the plate increases significantly with enrichment of the matrix with more CNT. Mechanical buckling analysis of functionally graded power-based and carbon nanotubes-reinforced composite plates and curved panels is studied by Zghal *et al.* (2018). Mohammadimehr *et al*. (2018c) investigated bending, buckling, and free vibration analyses of carbon nanotube reinforced composite beams and experimental tensile test to obtain the mechanical properties of nanocomposite. Dynamic analysis of functionally graded carbon nanotubes-reinforced plate and shell structures using a double director's finite shell element is studied by Frikha *et al*. (2018). Influence of material uncertainties on vibration and bending behaviour of skewed sandwich FGM plates is studied by Tomar and Talha (2019). They studied that coefficient of variance (COV) of transverse deflection increases with the increase in number of independent random variables. A modified first-order shear deformation theory (FSDT)-based four nodes finite shell element for thermal buckling analysis of functionally graded plates and cylindrical shells is performed by Trabelsi *et al*. (2019).

Bending analysis of sandwich plates with different face sheet materials and functionally graded soft core is performed by Li *et al.* (2018). The influences of volume fraction distribution, the thickness to side ratio and the layer thickness ratio on plate bending characteristics are studied in detail.

3D capability of refined GDQ models for the bending analysis of composite and sandwich plates, spherical and doubly-curved shells is studied by Tornabene and Brischetto (2018).

Thermo-electro-mechanical bending behavior of sandwich nanoplate integrated with piezoelectric face-sheets based on trigonometric plate theory is performed by Arefi and Zenkour (2017). Structural behavior of sandwich panels with asymmetrical boundary conditions studied by Studziński *et al.* (2015). Simulation of static behaviour of skew plates is an interesting area of work for the researchers. Joodaky and Joodaky (2015) studied a semi-analytical study on static behaviour of thin skew plates on elastic foundation. They obtained the governing equations of plate by using the classical plate theory. Using the Kantorovich method, the stresses of the plate were measured according to the angle of the skew plate and the stiffness of the springs.

Arani *et al*. (2017), Kolahdouzan *et al*. (2018) presented buckling and free vibration analysis of FG-CNTRC-micro sandwich plate and vibration analysis of functionally graded nanocomposite plate moving in two directions, respectively. Some studies investigated the surface and size dependent effect on the bending, buckling and vibration analysis of micro structures (Arani *and co-workers* 2015, Mohammadimehr *et al*. 2017b, 2018b, Bahaadini *et al*. 2019).

Some researchers works about buckling (Bilouei *et al*. 2016), vibration analysis of concrete columns and buckling of concrete columns retrofitted with Nano-Fiber Reinforced Polymer (NFRP) and pipes reinforced by SiO_2 nanoparticles, respectively. Also, Motezaker and Kolahchi (2017) presented seismic response of SiO_2 nanoparticles-reinforced concrete pipes based on DQ and newmark methods.

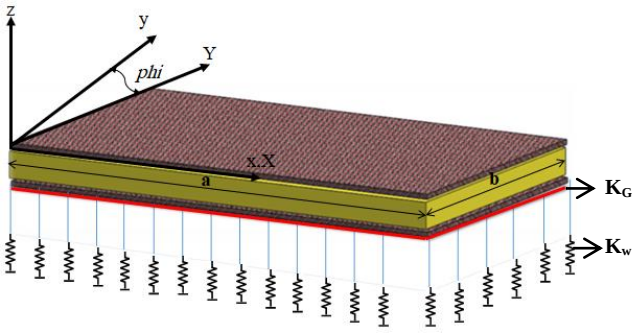

Fig. 1 Sandwich skew plate in oblique coordinate (*X*,*Y*) resting on the elastic foundations with the stiffness of *K* and reinforced by FG-SWCNTs

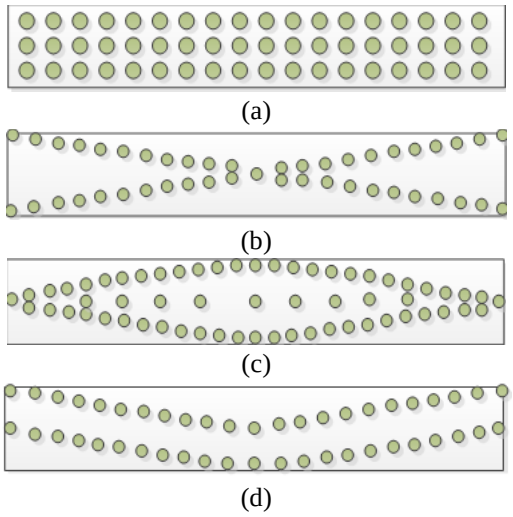

Fig. 2 Configurations of CNTs reinforced composite face sheets. (a) UD CNTRC (b) FG-X CNTRC (c) FG-O CNTRC (d) FG-V CNTRC

This study presents a semi analytical closed-form solution for governing equations of thin skew plates and micro sandwich skew plate with an isotropic core and functionally graded carbon nanotubes (FG-CNTs) reinforced nanocomposite face sheets. Single-walled carbon nanotubes (SWCNTs) with different distributions are employed to reinforce the micro sandwich skew plate. Effective materials properties of the nanocomposites are estimated using Eshelby-Mori-Tanaka approach. In this research, the various boundary conditions such as clamped, free and simply supported under uniform loading resting on the elastic foundations are considered. Classical plate theory (CPT) and modified strain gradient theory (MSGT) is used for modeling the thin skew plates and micro sandwich skew plate.

2. Geometry and simulation

A micro sandwich skew plate of length a and width b, resting on Winkler and Pasternak foundation is presented in Fig. 1. Furthermore, the coordinate axes for face sheets and core of foundation in Oblique coordinates (*X*,*Y*) are shown in Fig. 1.

The skew plate can be described by oblique coordinate *X*-*Y*. The skew angle of the plate (*phi or* (φ)) is measured with respect to the y-axis, as shown in the Fig. 1. The length and width of the skew plate in the *X* and *Y* directions are *a* and *b*, respectively. Also, K_w and K_G denote two parameters of elastic foundation. The relationship between the *x*-*y* coordinate and the *X*-*Y* coordinate can be written as $X=x-y\tan(\varphi)$ $Y=y/\cos(\varphi)$.

If *phi* angle is equal to zero, the skew plate is converted to rectangular plate.

Fig. 2 displays various distribution patterns of SWNTs in the nanocomposite plate. As it can be seen from this figure, these patterns are a) uniform distribution (UD), b) FG-X, c) FG-O d) FG-V, respectively. Volume fraction of various SWCNTs distribution patterns can be expressed as follows (Mohammadimehr *et al.* 2016)

$$V_{CNT}(z)=\begin{cases} V_{CNT}^{*} & (UD) \\ (1+\dfrac{2z}{h})V_{CNT}^{*} & (FG-V) \\ 2(1-\dfrac{|2z|}{h})V_{CNT}^{*} & (FG-O) \\ 2\dfrac{|2z|}{h}V_{CNT}^{*} & (FG-X) \end{cases} \tag{1}$$

where

$$V_{CNT}^{*}=\frac{w_{CNT}}{w_{CNT}+(\dfrac{\rho_{CNT}}{\rho_m})(1-w_{CNT})} \tag{2}$$

w_{CNT}, ρ_m and ρ_{CNT} are SWCNTs mass fraction, matrix density and SWCNTs density, respectively. Mass and volume of SWCNTs is same for four types of SWCNT distributions.

The face sheets and core are considered as thin plate, thus CPT is applied to model the face sheets and core in Eq. (3) and therefore the displacement fields are given as follows

$$\begin{cases} u(x,y,z)=u_0(x,y)-z\dfrac{\partial w(x,y)}{\partial x} \\ v(x,y,z)=v_0(x,y)-z\dfrac{\partial w(x,y)}{\partial y} \\ w(x,z,t)=w(x,y) \end{cases} \tag{3}$$

So the kinematic relations for the micro structher are considered the following form

$$\begin{cases} \varepsilon_{yy}=\dfrac{\partial}{\partial y}v(x,y,z) \\ \varepsilon_{xx}=\dfrac{\partial}{\partial x}u(x,y,z) \\ \gamma_{yx}=\dfrac{\partial}{\partial y}u(x,y,z)+\dfrac{\partial}{\partial x}v(x,y,z) \\ \gamma_{xz}=\gamma_{yz}=\varepsilon_{zz}=0 \end{cases} \tag{4}$$

The effective mechanical properties of the nanocomposite face sheets reinforced by single-walled carbon nanotubes are developed by employing the EMT approach. CNTs fibers are assumed to be straight and long

with UD in the isotropic matrix. According to EMT approach, the parameters from this theory have been defined as follows

$$\begin{cases} k = \dfrac{E_m\{E_m V_m + 2k_r(1+\upsilon_m)[1+V_{CNT}(1-2\upsilon_m)]\}}{2(1+\upsilon_m)\left[E_m(1+V_{CNT}-2\upsilon_m)+2V_m k_r(1-\upsilon_m-2\upsilon_m^2)\right]} \\ l = \dfrac{E_m\{V_m\upsilon_m[E_m+2k_r(1+\upsilon_m)]+2V_{CNT}l_r(1-\upsilon_m^2)\}}{(1+\upsilon_m)\left[E_m(1+V_{CNT}-2\upsilon_m)+2V_m k_r(1-\upsilon_m-2\upsilon_m^2)\right]} \\ n = \dfrac{E_m^2 V_m(1+V_{CNT}-V_m\upsilon_m)+2V_m V_{CNT}(k_r n_r - l_r^2)(1+\upsilon_m)^2(1-2\upsilon_m)}{(1+\upsilon_m)\left[E_m(1+V_{CNT}-2\upsilon_m)+2V_m k_r(1-\upsilon_m-2\upsilon_m^2)\right]} \\ \quad + \dfrac{E_m\left[2V_m^2 k_r(1-\upsilon_m)+V_{CNT}n_r(1+V_{CNT}-2\upsilon_m)-4V_m l_r\upsilon_m\right]}{E_m(1+V_{CNT}-2\upsilon_m)+2V_m k_r(1-\upsilon_m-2\upsilon_m^2)} \\ p = \dfrac{E_m\left[E_m V_m + 2p_r(1+\upsilon_m)(1+V_{CNT})\right]}{2(1+\upsilon_m)\left[E_m(1+V_{CNT})+2V_m p_r(1+\upsilon_m)\right]} \\ m = \dfrac{E_m\left[E_m V_m + 2m_r(1+\upsilon_m)(3+V_{CNT})-4\upsilon_m\right]}{2(1+\upsilon_m)\left\{E_m\left[V_m+4V_{CNT}(1-\upsilon_m)\right]+2V_m m_r(3-\upsilon_m-4\upsilon_m^2)\right\}} \end{cases} \tag{5}$$

where k is the plane-strain bulk modulus normal to the fiber direction l is the associated cross modulus, m and p are known as the shear moduli in planes normal and parallel to the fiber direction, respectively. These coefficients are called the Hill's elastic moduli for the CNTs. Also, the subscripts m and r represent the quantities of the matrix and the reinforcing phase, respectively. Also, E_m, υ_m, and V_m are the Young's modulus, the Poisson's ratio, and the volume fraction of the matrix, respectively. It is noted that these parameters have been used in Eq. (7) that the components of stiffness for composite facesheets have been obtained.

The mechanical and electrical properties of composite material which is presented by Akbari Alashti *et al*. (2012) is shown in Table 1.

k_r, l_r, m_r, n_r and p_r are the volume fraction and Hill's elastic modulus of the reinforcement for CNT in Table 2.

Also V_{CNT} and V_m are volume fraction of the nanotube and matrix, respectively and are related by the following form

$$V_m + V_{CNT} = 1 \tag{5}$$

Table 1 The mechanical, electrical properties of composite material (Akbari Alashti *et al.* 2012)

	Symbol	Unit of measurement	*PZT_4*
mechanical properties	υ	---	0.30
	ρ	Kg/m^3	7600
Elastic mechanical constants	C^*_{11}	GPa	139
	C^*_{12}	GPa	77.80
	C^*_{22}	GPa	115
	C^*_{44}	GPa	25.60
	C^*_{55}	GPa	25.60
	C^*_{66}	GPa	25.60
Piezoelectric constants	e^*_{31}	C/m^2	-5.20
	e^*_{32}	C/m^2	-5.20
	e^*_{33}	C/m^2	15.10
	η^*_{33}	nC^2/Nm^2	6.5

Table 2 The volume fraction and Hill's elastic modulus for SWCNTs

Elastic Constant	k_r	l_r	m_r	n_r	p_r
GPa	30	10	1	1	450

Finally, by combining the relationships (1) and (5) and (6) using the data of Tables 1 and 2, inserting the results obtained from them in Eshelby-Mori-Tanaka approach Eq. (8), the mechanical equivalent properties and electric for composite facesheets (Nasihatgozar 2016)

$$\begin{aligned} &c_{11} = k + m \quad c_{12} = l \quad c_{21} = l \quad c_{22} = n \quad c_{66} = p \quad c_{13} = k - m \\ &c_{33} = k + m \quad c_{32} = l \quad c_{23} = l \quad c_{31} = k - m \end{aligned} \tag{7}$$

$$\begin{aligned} &C_{11} = C^*_{11} - ((c_{13}{}^2)/c_{33}) \qquad C_{12} = C^*_{12} - ((c_{13}c_{23})/c_{33}) \\ &C_{21} = C^*_{21} - ((c_{13}c_{23})/c_{33}) \qquad C_{22} = C^*_{22} - ((c_{23}{}^2)/c_{33}) \\ &C_{66} = G_{12} \\ &\eta_{11} = \eta^*_{33} - ((c_{13}\cdot e^*_{33})/c_{33}) \\ &\eta_{22} = \eta^*_{33} - ((c_{13}\cdot e^*_{33})/c_{33}) \\ &\eta_{33} = \eta^*_{33} - ((c_{13}\cdot e^*_{33})/c_{33}) \\ &e_{31} = e^*_{31} - (c_{13}/c_{33})\cdot e^*_{33} \\ &e_{32} = e^*_{32} - (c_{23}/c_{33})\cdot e^*_{33} \end{aligned} \tag{6}$$

In Eq. (8), C, e and η are elastic, piezoelectric, and dielectric constants, respectively.

Using Hook's law, stress-strain relations for core can be stated as follows

$$\begin{cases} \sigma_{xx} = Q_{11}\varepsilon_{xx} + Q_{12}\varepsilon_{yy} \\ \sigma_{yy} = Q_{21}\varepsilon_{xx} + Q_{22}\varepsilon_{yy} \\ \sigma_{xy} = Q_{66}\gamma_{xy} \end{cases} \tag{7}$$

where σ_{ij} and ε_{ij} are the stress, strain components. Also, Q_{ij} is the reduced elastic constant for core which can be expressed as follows

$$\begin{aligned} &Q_{11} = \frac{E_{11}}{1-\nu_{12}\nu_{21}} \qquad Q_{22} = \frac{E_{22}}{1-\nu_{12}\nu_{21}} \\ &Q_{12} = \frac{\nu_{21}E_{11}}{1-\nu_{12}\nu_{21}} \qquad Q_{66} = G_{12} \\ &Q_{12} = Q_{21} \end{aligned} \tag{8}$$

In order to obtain the governing equations for sandwich skew plate with piezoelectric facesheet and composite-reinforced with carbon nanotubes, the principle of minimum potential energy is used. In this method, the total potential energy is obtained from the sum of the energy of the strain potential and the energy generated by the work of external forces in the following form

$$\prod = (U + V) \tag{9}$$

where U and V are strain energy and external work, respectively.

With the determination of the total potential energy and employing of the principle of minimum potential energy, we can derive the governing equations for the sandwich skew plate

$$\delta \prod = 0 \ \rightarrow \ \delta U + \delta V = 0 \tag{10}$$

Work done by the external loads can be stated as

$$\delta V = -\int_A \left\{ \left[K_w w(x,y) - K_G \left(\frac{\partial^2 w(x,y)}{\partial x^2} + \frac{\partial^2 w(x,y)}{\partial y^2} \right) \right] \delta w \right\} dA + \int_A [q \delta w] dA \tag{11}$$

where $q(x,y)$ is transverse load per length.

The variation of strain energy based on MSGT for the micro sandwich piezoelectric skew plate can be obtained as follows

$$\delta U = \int_{\forall} (\sigma_{ij} \delta \varepsilon_{ij} + p_i \delta \gamma_i + \tau_{ijk}^{(1)} \delta \eta_{ijk}^{(1)} + m_{ij}^{(s)} \delta \chi_{ij}^{(s)} - D_i \delta E_i) d\forall \tag{14}$$

where η_{ijk}, χ_{ij} and γ_i are deviatoric stretch gradient tensor, symmetric rotation gradient tensor and dilatation gradient vector, respectively, and D_i and E_i denote the electric displacement and the electric field, respectively, (that they can be obtained as the following form

$$\varepsilon_{ij} = \frac{1}{2} \left(\frac{\partial u_i(x,z,t)}{\partial x_j} + \frac{\partial u_j(x,z,t)}{\partial x_i} \right) \tag{15}$$

$$\gamma_i = \frac{\partial \varepsilon_{kk}}{\partial x_i} \tag{12}$$

$$\chi_{ij}^{(s)} = \frac{1}{2} \left(e_{ipq} \frac{\partial \varepsilon_{qj}}{\partial x_p} + e_{jpq} \frac{\partial \varepsilon_{qi}}{\partial x_p} \right) \tag{13}$$

$$\eta_{ijk}^{(1)} = \frac{1}{3}(\varepsilon_{jk,i} + \varepsilon_{ki,j} + \varepsilon_{ij,k}) - \frac{1}{15}\delta_{ij}(\varepsilon_{mm,k} + 2\varepsilon_{mj,m}) - \frac{1}{15}\delta_{jk}(\varepsilon_{mm,i} + 2\varepsilon_{mi,m}) - \frac{1}{15}\delta_{ki}(\varepsilon_{mm,j} + 2\varepsilon_{mj,m}) \tag{18}$$

$$\sigma_{ij} = Q_{ij}\varepsilon_{ij} - e^T E_i \tag{19}$$

$$P_i = 2Gl_0^2 \gamma_i \tag{20}$$

$$\tau_{ijk}^{(1)} = 2Gl_1^2 \eta_{ijk}^{(1)} \tag{21}$$

$$m_{ij}^{(s)} = 2Gl_2^2 \chi_{ij} \tag{22}$$

In the above relations, u_i represents the displacement field components, G the shear modulus, δ the Kronecker delta, and e_{ijk} permutation symbol, which, in accordance with Eq. (23), can take values of zero, 1, and −1. Also l_0, l_1 and l_2 known as three material length scale parameters are the length of a substance, whose values are according to Table 3 for classical, modified couple stress and modified strain gradient theories.

$$\begin{cases} e_{123} = e_{231} = e_{312} = 1 \\ e_{321} = e_{132} = e_{213} = -1 \end{cases} \tag{14}$$

Table 3 The values of the small-scale particle size of the material for classical, modified couple stress and modified strain gradient theories

Theory	l_0 (μm)	l_1 (μm)	l_2 (μm)
CPT	0	0	0
MCST	0	0	17.6
MSGT	17.6	17.6	17.6

$$\begin{cases} E_i = -\dfrac{\partial \tilde{\varphi}_E(x,y,z)}{\partial x_i} \\ D_i = e_{ij}\varepsilon_{ij} + \eta_i E_i \end{cases} \tag{15}$$

In the relation (24) e_{ij}, η_i and $\tilde{\varphi}_E(x,y,z)$ represent piezoelectric constants, dielectrics and electrical potential, respectively. Also, the electrical potential according to (25) can be defined as follows (Arefi and Zenkour 2017)

$$\tilde{\varphi}_E(x,y,z) = -\cos(\psi z)\varphi_E(x,y) \tag{16}$$

It should be noted that in the present paper, the electric field is assumed to be two dimensional in the longitudinal and transverse directions of each of the composite facesheet.

Finally, with the formation of relations related to the terms of stress and electrical displacement, and their placement in relation (26), first order changes of strain energy of micro sandwich skew plate with piezoelectric facesheet and composite reinforced nanotubes are defined. Due to the sandwich structure of the microstructure and the changes in their properties in each of the upper, lower and middle corners, the integral curves are divided into three parts, each of which represents the thicknesses of the diagonal micro-sheet layers.

$$\delta U = \int_A \left\{ \begin{array}{l} \left[\begin{array}{l} -\dfrac{\partial^2}{\partial x^2} M_{xx} - \dfrac{\partial^2}{\partial y^2} M_{yy} - 2\dfrac{\partial^2}{\partial y \partial x} M_{xy} + \dfrac{\partial^3}{\partial x^3} P_{1x} \\ + \dfrac{\partial^3}{\partial x \partial y^2} P_{1x} + \dfrac{\partial^3}{\partial x^2 \partial y} P_{1y} + \dfrac{\partial^3}{\partial y^3} P_{1y} - \dfrac{\partial^2}{\partial x^2} P_{0z} \\ - \dfrac{\partial^2}{\partial y^2} P_{0z} + \dfrac{2}{5}\dfrac{\partial^3}{\partial x^3} T_{1xxx} - \dfrac{3}{5}\dfrac{\partial^3}{\partial x \partial y^2} T_{1xxx} \\ + 3\left(\dfrac{4}{5}\dfrac{\partial^3}{\partial x^2 \partial y} T_{1xxy} - \dfrac{1}{5}\dfrac{\partial^3}{\partial y^3} T_{1xxy} \right) \\ + 3\left(-\dfrac{4}{15}\dfrac{\partial^2}{\partial x^2} T_{0xxz} + \dfrac{1}{15}\dfrac{\partial^2}{\partial y^2} T_{0xxz} \right) \\ + 6\left(\dfrac{-1}{3}\dfrac{\partial^2}{\partial x \partial y} T_{0xyz} \right) + 3\left(\dfrac{4}{5}\dfrac{\partial^3}{\partial x \partial y^2} T_{1xyy} - \dfrac{1}{5}\dfrac{\partial^3}{\partial x^3} T_{1xyy} \right) \\ + 3\left(-\dfrac{1}{5}\dfrac{\partial^3}{\partial x^3} T_{1xzz} - \dfrac{1}{5}\dfrac{\partial^3}{\partial x \partial y^2} T_{1xzz} \right) + \dfrac{2}{5}\dfrac{\partial^3}{\partial y^3} T_{1yyy} \\ - \dfrac{3}{5}\dfrac{\partial^3}{\partial x^2 \partial y} T_{1yyy} + 3\left(-\dfrac{4}{5}\dfrac{\partial^2}{\partial y^2} T_{0yyz} + \dfrac{1}{15}\dfrac{\partial^2}{\partial x^2} T_{0yyz} \right) \\ + 3\left(-\dfrac{1}{5}\dfrac{\partial^3}{\partial x^2 \partial y} T_{1yzz} - \dfrac{1}{5}\dfrac{\partial^3}{\partial y^3} T_{1yzz} \right) - \dfrac{1}{5}\dfrac{\partial^2}{\partial x^2} T_{0zzz} \\ - \dfrac{1}{5}\dfrac{\partial^2}{\partial y^2} T_{0zzz} + \dfrac{\partial^2}{\partial x \partial y} R_{0x} - \dfrac{\partial^2}{\partial x \partial y} R_{0y} - \dfrac{\partial^2}{\partial x^2} R_{0xy} \\ - \dfrac{\partial^2}{\partial y^2} R_{0xy} \end{array} \right] \delta w \\ + \left[\dfrac{\partial}{\partial x} D_{1x} + \dfrac{\partial}{\partial y} D_{1y} + D_{1z} \right] \delta \psi \end{array} \right\} dA \tag{17}$$

where the values for resultant forces and moments, higher order stresses, and electrical displacement are defined in Appendix A.

The governing equations of equilibrium can be derived by using the principle of minimum potential energy (Eq. (12)). Using Eqs. (26) integrating through the thickness of the plate by part and setting the coefficients of δw and $\delta\psi$ to zero separately, one can obtain the equilibrium equations associated with CPT theory as follows

$$\begin{aligned}
&\partial w: -\frac{\partial^2}{\partial x^2}M_{xx} - \frac{\partial^2}{\partial y^2}M_{yy} - 2\frac{\partial^2}{\partial y\partial x}M_{xu} + \frac{\partial^3}{\partial x^3}P_{1x} \\
&+ \frac{\partial^3}{\partial x\partial y^2}P_{1x} + \frac{\partial^3}{\partial x^2\partial y}P_{1y} + \frac{\partial^3}{\partial y^3}P_{1y} - \frac{\partial^2}{\partial x^2}P_{0z} - \frac{\partial^2}{\partial y^2}P_{0z} \\
&+ \frac{2}{5}\frac{\partial^3}{\partial x^3}T_{1xxx} - \frac{3}{5}\frac{\partial^3}{\partial x\partial y^2}T_{1xxx} \\
&+ 3\left(\frac{4}{5}\frac{\partial^3}{\partial x^2\partial y}T_{1xxy} - \frac{1}{5}\frac{\partial^3}{\partial y^3}T_{1xxy}\right) + 3\left(-\frac{4}{15}\frac{\partial^2}{\partial x^2}T_{0xxz} + \frac{1}{15}\frac{\partial^2}{\partial y^2}T_{0xxz}\right) \\
&+ 6\left(\frac{-1}{3}\frac{\partial^2}{\partial x\partial y}T_{0xyz}\right) + 3\left(\frac{4}{5}\frac{\partial^3}{\partial x\partial y^2}T_{1xyy} - \frac{1}{5}\frac{\partial^3}{\partial x^3}T_{1xyy}\right) \\
&+ 3\left(-\frac{1}{5}\frac{\partial^3}{\partial x^3}T_{1xzz} - \frac{1}{5}\frac{\partial^3}{\partial x\partial y^2}T_{1xzz}\right) + \frac{2}{5}\frac{\partial^3}{\partial y^3}T_{1yyy} - \frac{3}{5}\frac{\partial^3}{\partial x^2\partial y}T_{1yyy} \\
&+ 3\left(-\frac{4}{5}\frac{\partial^2}{\partial y^2}T_{0yyz} + \frac{1}{15}\frac{\partial^2}{\partial x^2}T_{0yyz}\right) + 3\left(-\frac{1}{5}\frac{\partial^3}{\partial x^2\partial y}T_{1yzz} - \frac{1}{5}\frac{\partial^3}{\partial y^3}T_{1yzz}\right) \\
&- \frac{1}{5}\frac{\partial^2}{\partial x^2}T_{0zzz} - \frac{1}{5}\frac{\partial^2}{\partial y^2}T_{0zzz} + \frac{\partial^2}{\partial x\partial y}R_{0x} - \frac{\partial^2}{\partial x\partial y}R_{0y} \\
&- \frac{\partial^2}{\partial x^2}R_{0xy} + \frac{\partial^2}{\partial y^2}R_{0xy} - K_G\cdot\frac{\partial^2}{\partial x^2}w(x,y,t) - K_G\cdot\frac{\partial^2}{\partial y^2}w(x,y,t) \\
&+ K_w\cdot w(x,y,t) - q(x,y) = 0 \\
&\partial\psi: \frac{\partial}{\partial x}D_{1x} + \frac{\partial}{\partial y}D_{1y} + D_{1z} = 0
\end{aligned} \tag{18}$$

Governing equations of (27) must be converted from Cartesian coordinates system (x,y) to Oblique coordinates system (X,Y) as it is shown in Fig. 1. The relations between Cartesian (x,y) and Oblique (X,Y) are

$$X = x - y\tan(\varphi) \tag{19}$$

$$Y = y/\cos(\varphi) \tag{20}$$

3. Iterative Solution by Kantorovich method

3.1 Classical plate at macro scale

In the present study, solving differential equations governing the micro sandwich skew plate has been used a semi-analytic method solution of (EKM). This method is one of the semi-analytic methods for solving various differential equations with partial derivatives. In this study, based on the classical theory of plates, the application of this method, along with the application of the Galerkin method .

The governing fourth-order partial differential equation (PDE) for skew plate and sixth -order partial differential equation (PDE) for micro sandwich skew plate, there are two-variable function of deflection, $w(X,Y)$, is defined in oblique coordinates system. Application of EKM together with the idea of weighted residual technique, converts the fourth and sixth-order governing equation to two ODEs in terms of X and Y in oblique coordinates. Both resulted ODEs, are then solved iteratively in a closed-form manner with a very fast convergence.

Finally deflection function is obtained. It is shown that some parameters such as angle of skew plate and stiffness of elastic foundation have an important effect on the results. Comparisons of the deflection at the various points of the plates show very good agreement with results of other analytical and numerical analyses.

To explain this method, the simplicity of the description is ignored by the sandwich and the micro-state.

$$\begin{aligned}
&\frac{D}{\cos^4(\varphi)}\left\{\frac{\partial^4 w(X,Y)}{\partial X^4} + 2(1+2\sin^2(\varphi))\frac{\partial^4 w(X,Y)}{\partial Y^2\partial X^2}\right. \\
&\left. - 4\sin(\varphi)\left(\frac{\partial^4 w(X,Y)}{\partial Y\,\partial X^3} + \frac{\partial^4 w(X,Y)}{\partial Y^3\partial X}\right) + \frac{\partial^4 w(X,Y)}{\partial Y^4}\right\} \\
&+ K_w w(X,Y) - K_G\frac{1}{\cos(\varphi)}\left(\frac{\partial^2 w(X,Y)}{\partial X^2} + \frac{\partial^2 w(X,Y)}{\partial Y^2}\right. \\
&\left. - 2\sin(\varphi)\frac{\partial^2 w(X,Y)}{\partial Y\,\partial X}\right) - q(X,Y) = 0
\end{aligned} \tag{21}$$

In this method, the multi-variable function of the multiplicative function is considered first from the variables in the main function, as follows.

$$w(X,Y) = f(X).g(Y) \tag{22}$$

Initially, one of the functions is assumed to be definite and a function is guessed for it.

Then, relation (30) and (31) is placed in the relation of the remaining weighting method (Galerkin), which, with the recent assumption that one of the functions of the relationship is known to be simpler, leads to the obtaining of one of the ordinary differential equations, which simplicity is solvable.

By solving this equation, another function is obtained, repeated this time with the function obtained, and another differential equation is obtained in terms of the same function as it was originally found to be.

Eventually, this repetition takes place so that the necessary convergence is achieved.

According to the description of the function of the Extended Kantorovich method (EKM), by substituting Eq. (31) into Eq. (30) yields the following equation

$$\begin{aligned}
&(\cos^4(\varphi)).\nabla^4(f(X).g(Y)) + \frac{K_w\cos^4(\varphi)}{D}f(X).g(Y)) \\
&- \frac{K_G\cos^3(\varphi)}{D}\left(\frac{\partial^2}{\partial X^2}(f(X).g(Y)) - \right. \\
&\left. 2\sin(\varphi)\frac{\partial^2}{\partial X\,\partial Y}(f(X).g(Y)) + \frac{\partial^2}{\partial Y^2}(f(X).g(Y))\right. \\
&= \left\{g(Y)\frac{d^4 f(X)}{dX^4} + 2(1+2\sin^2(\varphi))\frac{d^2 g(Y)}{dY^2}\frac{d^2 f(X)}{dX^2} - \right. \\
&\left. 4\sin(\varphi)\left(\frac{d\,g(Y)}{dY}\frac{d^3 f(X)}{dX^3} + \frac{d^3 g(Y)}{dY^3}\frac{d\,f(X)}{dX}\right)\right.
\end{aligned}$$

$$+\frac{d^4g(Y)}{dY^4}f(X)\Big\}+\frac{K_w\cos^4(\varphi)}{D}f(X).g(Y))-$$
$$\frac{K_G\cos^3(\varphi)}{D}\Big(g(Y)\frac{d^2f(X)}{dX^2}-2\sin(\varphi)\frac{d\,g(Y)}{dY}\frac{d\,f(X)}{dX}$$
$$+f(X)\frac{d^2g(Y)}{dY^2}\Big)=\frac{\cos^4(\varphi)}{D}q(X,Y) \tag{23}$$

According to the Galerkin weighted residual method, we have

$$\int_{-a}^{a}\int_{-b}^{b}\left(D\nabla^4w-q+K_ww-K_G\nabla^2w\right)\delta w\,dX\,dY=0 \tag{24}$$

Now, for a prescribed function of $g(Y)$ and referred to the Eq. (34), δwbecomes

$$\delta w=g(Y).\delta f(x) \tag{25}$$

Substituting Eq. (31) into Eq.(33) in conjunction with Eq. (34) leads to the following equation

$$\int_{-a}^{a}\left[\int_{-b}^{b}\left(D\nabla^4(f.g)-q+K_w(f.g)-K_G\nabla^2(f.g)\right)g\,dY\right]\delta f\,dX=0 \tag{35}$$

Based on the existing rules in the Variational principle, Eq. (35) is satisfied if the expression in the bracket is vanished

$$\int_{-b}^{b}\left(D\nabla^4(f.g)-q+K_w(f.g)-K_G\nabla^2(f.g)\right)g\,dY=0 \tag{36}$$

Now, with the integration of Eq. (36) and using the function for the initial conjecture, we can calculate the constants A_i (i=0: 6), and Eq. (36) converts to a fourth order equation.

$$A_4\frac{d^4f(X)}{dX^4}+A_3\frac{d^3f(X)}{dX^3}+A_2\frac{d^2f(X)}{dX^2}$$
$$+A_1\frac{d\,f(X)}{dX}+(A_0+A_5)f(X)=A_6 \tag{26}$$

The sides of the Eq. (37) are divided into A_4

$$\frac{d^4f(X)}{dX^4}+\frac{A_3}{A_4}\frac{d^3f(X)}{dX^3}+\frac{A_2}{A_4}\frac{d^2f(X)}{dX^2}$$
$$+\frac{A_1}{A_4}\frac{d\,f(X)}{dX}+\frac{(A_0+A_5)}{A_4}f(X)=\frac{A_6}{A_4} \tag{27}$$

In the following, the characteristic equation for equation (38) is obtained as follows

$$m^4+\frac{A_3}{A_4}m^3+\frac{A_2}{A_4}m^2+\frac{A_1}{A_4}m+\frac{(A_0+A_5)}{A_4}=0 \tag{28}$$

Eq. (39) consists of two parts, which have two private and general solutions.

The characteristic equation also has four mixed roots $m_r=\pm a_1\pm b_1 i$ r=1:4. Therefore, the general solution of the equation is equal to relation (40)

$$f(X)=e^{a_1X}\left(C_1\cos(b_1X)+C_2\sin(b_1X)\right)$$
$$)+e^{-a1X}\left(C_3\cos(b_1X)+C_4\sin(b_1X)\right)+C_5 \tag{29}$$

Table 4 Types of boundary conditions

boundary conditions	Equations satisfying boundary conditions in different situations
SSSS	$f(X)=\frac{d^2f(X)}{dX^2}=0$ for X=a , X=-a $g(Y)=\frac{d^2g(Y)}{dY^2}=0$ for Y=b , Y=-b
CCCC	$f(X)=\frac{df(X)}{dX}=0$ for X=a , X=-a $g(Y)=\frac{dg(Y)}{dY}=0$ for Y=b , Y=-b
CFCF	$f(X)=\frac{df(X)}{dX}=0$ for X=a , X=-a $g(Y)=\frac{d^3g(Y)}{dY^3}=0$ for Y=b , Y=-b
SFSF	$f(X)=\frac{d^2f(X)}{dX^2}=0$ for X=a , X=-a $g(Y)=\frac{d^3g(Y)}{dY^3}=0$ for Y=b , Y=-b

In the equation, C_5 answers the partial part which is considered equal to $\frac{A_6}{(A_0+A_5)}$ according to Eq. (39). To obtain the coefficients of C_i i=1:5, boundary conditions must be checked According to the Table 4.

By solving the Eq. (40), the first function $f(X)$ is obtained. Now, we continue the process of solving the equations, and by putting the $f(X)$ function as the second guess, the new δw form is obtained as (41)

$$\delta w=f(X).\delta g \tag{30}$$

The Galerkin equation is again written as follows

$$\int_{-a}^{a}\Big[\int_{-b}^{b}\left(D\nabla^4(f.g)-q+K_w(f.g)\right.$$
$$\left.-K_G\nabla^2(f.g)\right)f\;dX\Big]\delta g\;dY=0 \tag{31}$$

To satisfy the equation (42), the bracket should be zero. Using the obtained function for $f(X)$ and its integration in the above equation with X being taken into the second quadratic equationODE with respect to $g(Y)$ to obtain the function $g(Y)$ is equal to

$$B_4\frac{d^4g(Y)}{dY^4}+B_3\frac{d^3g(Y)}{dY^3}+B_2\frac{d^2g(Y)}{dY^2}$$
$$+B_1\frac{d\,g(Y)}{dY}+(B_0+B_5)g(Y)=B_6 \tag{32}$$

The characteristic equation for equation (43) is equal to

$$n^4+\frac{B_3}{B_4}n^3+\frac{B_2}{B_4}n^2+\frac{B_1}{B_4}n+\frac{(B_0+B_5)}{B_4}=0 \tag{33}$$

Again, by solving the characteristic equation, we obtain four roots $n_k=\pm a_2\pm b_2 i$ k=1 to 4, so $g(Y)$ is represented by the relation (2-35)

$$g(Y)=e^{a_2Y}\left(D_1\cos(b_2Y)+D_2\sin(b_2Y)\right)+e^{-a_2Y}$$
$$\left(D_3\cos(-b_2Y)+D_4\sin(-b_2Y)\right)+D_5 \tag{45}$$

Private answer is $D_5 = \frac{B_6}{(B_0 + B_5)}$.

This process continues by solving the equation *r* for new boundary conditions and obtaining the new *q* conjecture function. To obtain the *w*(*X*,*Y*) skew plate deflection function, the solving process continues until a reasonable convergence is obtained.

4. Micro sandwich skew plate

Previously, the use of this solving method has been described in the detailed equations. In this section, using the previous description of Eq. (27), it is rewritten to use in this method.

$$\ddot{\ddot{A}}_6 \frac{d^6 f(X)}{dX^6} + \ddot{\ddot{A}}_5 \frac{d^5 f(X)}{dX^5} + \ddot{\ddot{A}}_4 \frac{d^4 f(X)}{dX^4} + \ddot{\ddot{A}}_3 \frac{d^3 f(X)}{dX^3} + \ddot{\ddot{A}}_2 \frac{d^2 f(X)}{dX^2} + \ddot{\ddot{A}}_1 \frac{d f(X)}{dX} + \ddot{\ddot{A}}_0 f(X) = \ddot{\ddot{B}} \quad (34)$$

The coefficients $\ddot{\ddot{A}}_i$ $i = 0:6$ are explained in Appendix A. By dividing the relationship (46) into $\ddot{\ddot{A}}_6$, the equation for the characteristic of the above equation is written as follows

$$m_6 + \frac{\ddot{\ddot{A}}_5}{\ddot{\ddot{A}}_6} m_5 + \frac{\ddot{\ddot{A}}_4}{\ddot{\ddot{A}}_6} m_4 + \frac{\ddot{\ddot{A}}_3}{\ddot{\ddot{A}}_6} m_3 + \frac{\ddot{\ddot{A}}_2}{\ddot{\ddot{A}}_6} m_2 + \frac{\ddot{\ddot{A}}_1}{\ddot{\ddot{A}}_6} m_1 + \frac{\ddot{\ddot{A}}_0}{\ddot{\ddot{A}}_6} = 0 \quad (35)$$

By solving the characteristic Eq. (47), six roots are obtained. The solution of the above equation is presented as the sum of the private and public answers in the form of relation (48)

$$\tilde{f}(X) = \begin{cases} C_i e^{a_i X} \\ C_i e^{a_i X} \sin(b_i X) \\ C_i e^{a_i X} \cos(b_i X) \end{cases} \quad i = 1:6$$

$$f(X) = \frac{\ddot{B}}{A_0} + \tilde{f}(X) \quad (36)$$

In the relation (48), the coefficients C_i *i*=1:6 are obtained according to the boundary conditions of the problem. After determining this constancy and obtaining the general answer, this answer is used as a new conjecture, and this response time is obtained in terms of the Y variable. The rise of the problem is the product of *W*(*X*,*Y*)=*f*(*X*)*g*(*Y*). A fixed point is obtained at each calculation of a given function. This repetition continues until the desired convergence is achieved. The guessing functions in this section are presented in Appendix A.

Fig. 3 shows the convergence of the Kantorovich method in deflection of micro sandwich skew plate method that in this paper is accomplished at an acceptable rate in two steps. But for more certainty it's done in four steps.

5. Results and discussion

Consider a micro sandwich skew plate resting on the Winkler-Pasternak foundation as Fig. 1. The plate is subjected to a uniform loading and different combinations of clamped, free and simply supported boundary conditions for skew plate.

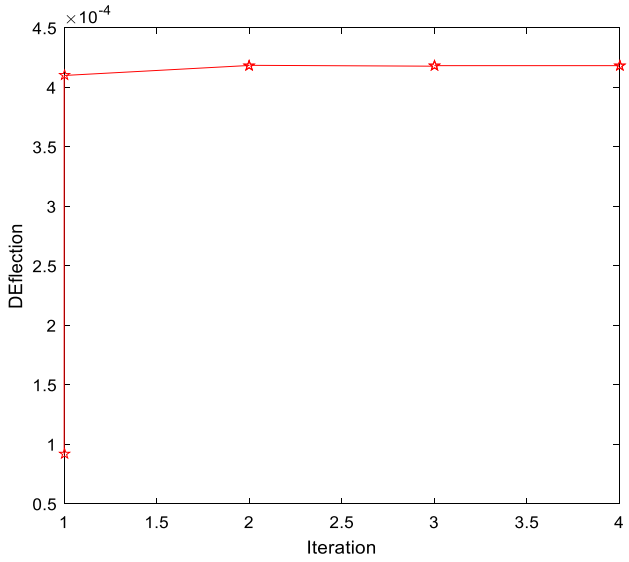

Fig. 3 Convergence of the Kantorovich method in deflection of micro sandwich skew plate

Table 5 The mechanical properties and geometry of the skew plate on elastic foundation

Properties of Stainless Steel 304								
a	*b*	*h*	*υ*	*ϕ*	K_w	K_G	q_0	*E*
0.5	0.5	0.02	0.25	20°	1×10^6 Pa/m	1×10^5 Pa.m	1×10^4 Pa	193 GPa

Table 6 The obtained results of the skew plate for various boundary conditions

Bounday Conditns	Iterations		
	1	2	3
CCCC	0.4523×10^{-4} 0.6495×10^{-4}	0.6698×10^{-4} 0.6703×10^{-4}	0.6703×10^{-4} 0.4703×10^{-4}
SSSS	0.05747×10^{-3} 0.1879×10^{-3}	0.1977×10^{-3} 0.1978×10^{-3}	0.1978×10^{-3} 0.1978×10^{-3}
SCFC	0.0601×10^{-3} 0.1077×10^{-3}	0.1079×10^{-3} 0.1079×10^{-3}	0.1079×10^{-3} 0.1079×10^{-3}
SCSC	0.5747×10^{-4} 0.9757×10^{-4}	0.9949×10^{-4} 0.9953×10^{-4}	0.9953×10^{-4} 0.9953×10^{-4}
CFCF	0.0452×10^{-3} 0.1081×10^{-3}	0.1164×10^{-3} 0.1160×10^{-3}	0.1160×10^{-3} 0.1160×10^{-3}

The initial guess of $g(Y)=(Y^2-b^2)^2$ and $g(Y)=(Y^2-b^2)^8$ for skew plate and micro sandwich skew plate respectively that does not satisfy all boundary conditions necessarily, is considered.

Table 5 presented the mechanical properties and geometry of the skew plate on elastic foundation.

In Table 6, a plate of stainless steel 304 with the characteristics of the Table 5 is presented for a variety of boundary conditions. All diagrams are shown inversely along *z* direction. When the skew angle is equaled to zero, the results can be employed for rectangular plates. The angle of skew plate in Fig. 4 and Table 6 is considered as 20°. It is shown from this Table that after third interation,

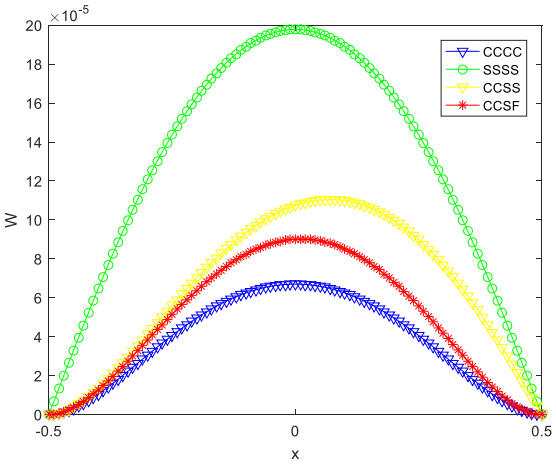

Fig. 4 Deflection of the skew plate for various boundary conditions

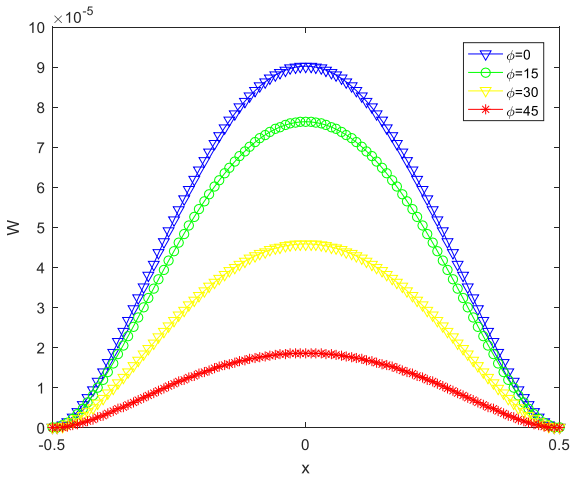

Fig. 5 The deflection of skew plate for various skew angles (φ)

Table 7 The mechanical properties of the core made of soft materials

E (GPa)	G (GPa)	υ	ρ (KG/m^3)	Q_{11}, Q_{22} (GPa)	Q_{12} (GPa)	Q_{44}, Q_{55}, Q_{66} (GPa)
130	22.05	0.27	60	60.40	16.31	22.05

the obtained results are convergence for deflection of skew plate based on various boundary conditions.

The effect of various boundary conditions such as SSSS, CCCC, CCSS, and CCSF on the deflection of skew plate is investigated in Fig. 4. It is shown that the greatest and lowest deflection is related to all edges simply supported (SSSS) and clamped (CCCC) boundary conditions, respectively. In this figure, it can be seen that the maximum deflection of skew plate does not occur in the center of the sheet for *CCSS* and *CCSF* states.

Fig. 5 shows the effect of various skew angles (φ) on the deflection results of CCCC skew plate. As can be seen, with the increase in the angle of the sheet, the amount of heights in the center decreases.

The mechanical properties of the micro sandwich skew plate for facesheet are given in Table 1 and for the core

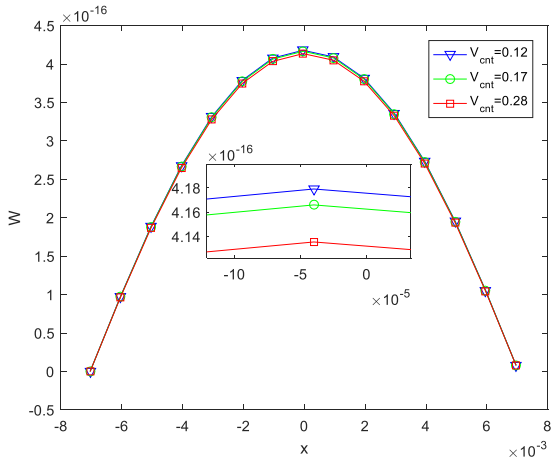

Fig. 6 Variation of deflection of the micro sandwich skew plate with different values of CNTs volume fraction (SSSS)

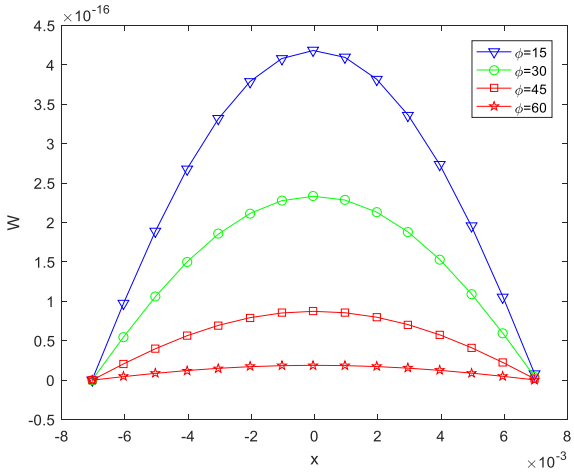

Fig. 7 Deflection of the *SSSS* micro sandwich skew plate, for various skew angles of φ

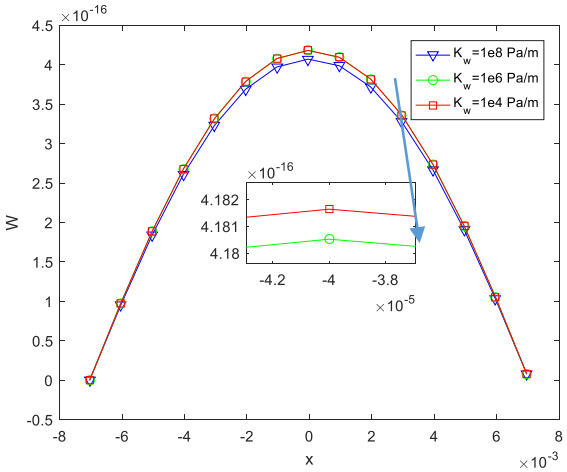

Fig. 8 The effect of Winkler's spring coefficient on the deflection of micro sandwich skew plate for φ=15°

according to Table 7. The geometric characteristics of the micro sandwich skew plate are also explained as follows:

As shown in Fig. 6, with an increase in the volume fraction of carbon nanotube, the deflection of the micro

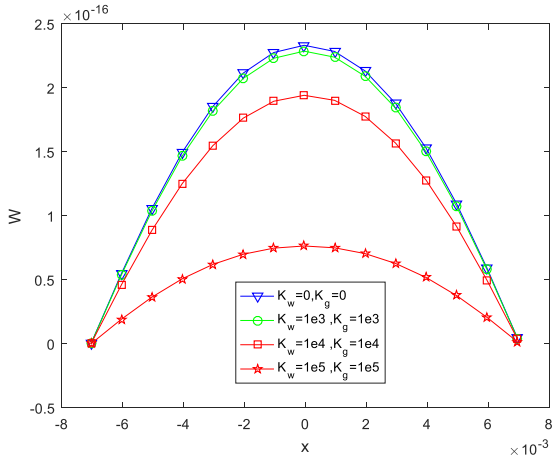

Fig. 9 Deflection of the SSSS micro sandwich skew plate for various elastic foundation along the $Y=b$ and X axes

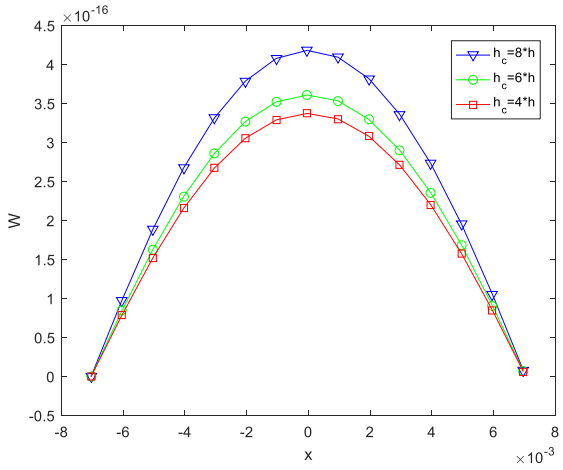

Fig. 10 The effect of the thickness of the core on the deflection of micro sandwich skew plate at φ=15°

sandwich skew plate decreases.

Fig. 7 shows the effect of the angle φ on the deflection of the skew microstructure. As can be seen, by increasing the angle of the skew plate, the deflection of the microstructure decreases. To the extent that ϕ=60° upwards changes do not occur.

Fig. 8 depicts the effect of Winkler's spring coefficient on the deflection of micro sandwich skew plate for φ=15°. It is shown from this figure that with an increase in Winkler's spring coefficient due to enhancing stiffness of micro structures, the deflection of micro sandwich skew plate reduces. It is evident in this diagram that the micro sandwich structure does not change much in stiffness of K_w=1×10^6 Pa/m and the rate of change is less dependent on the deflection, while the effective changes occur in K_w=1×10^8 Pa/m later.

The effect of shear constant of elastic foundation on micro structures is more than the spring constant that is shown in Fig. 9.

Fig. 10 shows an increase in the thickness of the core and its effect on the deflection. It is seen that by increasing the thickness of the core (the thickness of the facesheet decreases due to the total thickness is constant), the

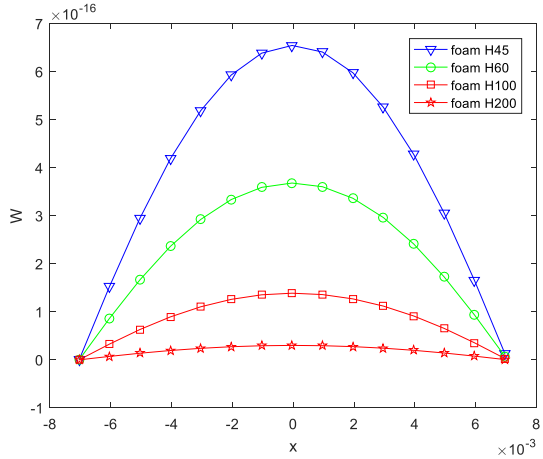

Fig. 11 The effect of various foam materials for the core

Table 8 Comparison of results for Kantorovich and Navier's methods

Deflection \ Solving method	*EKM*	*Navier*
	0.44528×10^{-3}	0.43041×10^{-3}

Table 9 Comparison of the results for the skew plate

Boundary conditions	Deflection(m)	
	Joodaky and Joodaky (2015)	Present work
CCCC	0.1882×10^{-2}	0.1881×10^{-2}
SCSC	0.3179×10^{-2}	0.3179×10^{-2}

deflection of micro sandwich plate increases.

Fig. 11 shows the effect of various foam materials for the core on the deflection of micro sandwich skew plate. By increasing the elasticity modulus for various foam core, from *Foam H*45 to *Foam H*200, the deflection of micro structure decreases.

The obtained results by Kantorovich method is compared with the presented results by Naviers's type solution in Table 8. It is shown that they have a good agreement between them for φ=0, q=1000 and K_w=1e^6.

The obtained results from this research has been compared the presented results by Joodaky and Joodaky (2015) for two cases boundary conditions in Table 9. It is seen that they have a good agreement each other for φ=0, q=1000 and K_w=1e^6.

6. Conclusions

In this research, bending analysis of micro sandwich skew plate with isotropic core and piezoelectric composite face sheets reinforced by carbon nanotube on the elastic foundations was studied. The classical plate theory (CPT) was used to model micro sandwich skew plate and to apply size dependent effects based on modified strain gradient theory. Eshelby-Mori-Tanaka approach is considered for the effective mechanical properties of the nanocomposite face sheets. The governing equations of equilibrium are derived using minimum principle of total potential energy and then solved by extended Kantorovich method (EKM). The some

important results from this research has been presented as follows:

1. The Kantorovich method is suitable for obtaining a deflection of plate and skew plate. Using this method, we can calculate the plate deflection for a variety of simply supported, clamped, and free boundary conditions. This method is very suitable for solving two-dimensional problems in comparison with other methods, such as limiting elements and differential squares. Appropriate convergence of this method occurs in three stages. It can be seen that this method has the best convergence in lower iterations.
2. This method is suitable for solving lower-order equations. By increasing the equation and increasing the boundary conditions, the quality of this method is reduced.
3. The effect of the angle of the micro sandwich skew plate shows that with increasing the amount of it, the deflection of micro-plate decreases and the increase in the thickness of the core, the deflection of micro sandwich structures increases.
4. In a survey on a variety of boundary conditions and its effect on the deflection of the microstructure, it is shown that the maximum point of deflection is not in the non-symmetric boundary conditions in the center of the plate.
5. The effect of various boundary conditions such as SSSS, CCCC, CCSS, and CCSF on the deflection of skew plate is investigated in this research. It is shown that the greatest and lowest deflection is related to all edges simply supported (SSSS) and clamped (CCCC) boundary conditions, respectively. It can be seen that the maximum deflection of skew plate does not occur in the center of the sheet for CCSS and CCSF states.
6. The effect of various foam materials for the core on the deflection of micro sandwich skew plate is presented. It is seen that by increasing the elasticity modulus for various foam core, from *Foam H*45 to *Foam H*200, the deflection of micro structure decreases.
7. The effect of shear constant of elastic foundation on micro structures is more than the spring constant.

Acknowledgment

The authors would like to grateful to the Iranian Nanotechnology Development Committee for their financial support and the University of Kashan for supporting this work by Grant No. 682561/27.

References

Abouhamze, M., Aghdam, M.M. and Alijani, F. (2007), "Bending analysis of symmetrically laminated cylindrical panels using the extended Kantorovich method", *Mech. Adv. Mater. Struct.*, **14**(7), 523-530. https://doi.org/10.1080/15376490701585967.

Aghdam, M.M. and Mohammadi, M. (2009), "Bending analysis of thick orthotropic sector plates with various loading and boundary conditions", *Compos. Struct.*, **88**, 212-218. https://doi.org/10.1016/j.compstruct.2008.03.038.

Aghdam, M.M., Mohammadi, M. and Erfanian, V. (2007), "Bending analysis of thin annular sector plates using extended Kantorovich method", *Thin Wall. Struct.*, **45**, 983-990. https://doi.org/10.1016/j.tws.2007.07.012.

AkbariAlashti, R. and Khorsand, M. (2012) "Tree-dimensional dynamo-thermo-elastic of a functionally graded cylindrical shell with piezoelectric layers by DQ-FD coupled", *Int. J. Press. Ves. Pip.*, **97**, 49-67. https://doi.org/10.1016/j.ijpvp.2012.06.006.

Alibeigloo, A. and Tahrimaslak, A. (2018), "Three dimensional transient analysis of FGM rectangular sandwich late subjected to thermal loading", *12th International Conference on Sandwich Structures*, Lausanne, Switzerland, August.

Arani, A.G., Haghparast, E. and Zarei, H.B. (2017), "Vibration analysis of functionally graded nanocomposite plate moving in two directions", *Steel Compos. Struct.*, **23**(5), 529-541. https://doi.org/10.12989/scs.2017.23.5.529.

Arani, A.G., Hashemian, M., Loghman, A. and Mohammadimehr, M. (2011b), "Study of dynamic stability of the double-walled carbon nanotube under axial loading embedded in an elastic medium by the energy method", *J. Appl. Mech. Tech. Phys.*, **52**(5), 815-824. https://doi.org/10.1134/S0021894411050178.

Arani, A.G., Mobarakeh, M.R., Shams, S. and Mohammadimehr, M. (2012), "The effect of CNT volume fraction on the magneto-thermo-electro-mechanical behavior of smart nanocomposite cylinder", *J. Mech. Sci. Technol.*, **26**(8), 2565-2572. https://doi.org/10.1007/s12206-012-0639-5.

Araújo, A.L., Carvalho, V.S., Soares, C.M., Belinha, J. and Ferreira, A.J.M. (2016), "Vibration analysis of laminated soft core sandwich plates with piezoelectric sensors and actuators", *Compos Struct.*, **151**, 91-98. https://doi.org/10.1016/j.compstruct.2016.03.013.

Arefi, M. and Zenkour, A.M. (2017), "Thermo-electro-mechanical bending behavior of sandwich nanoplate integrated with piezoelectric face-sheets based on trigonometric plate theory", *Compos. Struct.*, **162**, 108-122. https://doi.org/10.1016/j.compstruct.2016.11.071.

Bahaadini, R., Saidi, A.R. and Hosseini, M. (2019) "Flow-induced vibration and stability analysis of carbon nanotubes based on the nonlocal strain gradient Timoshenko beam theory", *J. Vib. Control*, **25**(1), 203-218. https://doi.org/10.1177/1077546318774242.

Bilouei, B.S., Kolahchi, R. and Bidgoli, M.R. (2016), "Buckling of concrete columns retrofitted with Nano-Fiber Reinforced Polymer (NFRP)", *Comput. Concrete*,**18**(5), 1053-1063. https://doi.org/10.12989/cac.2016.18.5.1053.

Calleja, M., Kosaka, P., San Paulo, A. and Tamayo, J. (2012), "Challenges for nanomechanical sensors in biological detection", *Nanoscale*, **49**(4), 25-38. DOI: 10.1039/C2NR31102J.

Frikha, A., Zghal, S. and Dammak, F. (2018), "Dynamic analysis of functionally graded carbon nanotubes-reinforced plate and shell structures using a double directors finite shell element", *Aerosp. Sci. Technol.*, **78**, 438-451. https://doi.org/10.1016/j.ast.2018.04.048.

Ghorbanpour Arani, A., Mohammadimehr, M., Saidi, A.R., Shogaei, S. and Arefmanesh, A. (2011a), "Thermal buckling analysis of double-walled carbon nanotubes considering the small-scale length effect", *Proc. Inst. Mech. Eng., Part C: J. Mech. Eng. Sci.*, **225**(1), 248-256. https://doi.org/10.1177/09544062JMES1975.

Jana, P. and Bhaskar, K. (2006), "Stability analysis of simply-supported rectangular plates under nonuniform uniaxial compression using rigorous and approximate plane stress solutions", *Thin Wall. Struct.*, **44**, 507-516. https://doi.org/10.1016/j.tws.2006.04.009.

Jia, Y. and Sun, K. (2006), "Thick film wireless and powerless strain sensor", *Smart Struct. Mater.*, **6174**, 299-309.

https://doi.org/10.1117/12.660365.
Jones, R. and Milne, B.J. (1976), "Application of extended Kantorovich method to the vibration of clamped rectangular plates", *J. Sound Vib.*, **45**(3), 309-316. https://doi.org/10.1016/0022-460X(76)90390-4.
Joodaky, A. and Joodaky, I. (2015), "A semi-analytical study on static behavior of thin skew plates on Winkler and Pasternak foundation", *Int. J. Mech. Sci.*, **100**, 322-327. https://doi.org/10.1016/j.ijmecsci.2015.06.025.
Kantorovich, L.V. and Krylov, V.I. (1960), "Approximate method of higher analysis", *Soc. Indus. Appl. Math.*, **2**(4), 299-300. https://doi.org/10.1090/S0002-9904-1960-10408-9.
Kiani, Y. and Mirzaei, M. (2018), "Rectangular and skew shear buckling of FG-CNT reinforced composite skew plates using Ritz method", *Aerosp. Sci. Technol.*, **77**, 388-398. https://doi.org/10.1016/j.ast.2018.03.022.
Kim, H.S., Cho, M. and Kim, G.I.. (2000), "Free-edge strength analysis in composite laminates by the extended Kantorovich method", *Compos. Struct.*, **49**, 229-235. https://doi.org/10.1016/S0263-8223(99)00138-5.
Kolahdouzan, F., Arani, A.G. and Abdollahian, M. (2018), "Buckling and free vibration analysis of FG-CNTRC-micro sandwich plate", *Steel Compos. Struct.*, **26**(3), 273-287. https://doi.org/10.12989/scs.2018.26.3.273.
Li, D., Deng, Z., Xiao, H. and Peng, J. (2018), "Bending analysis of sandwich plates with different face sheet materials and functionally graded soft core", *Thin Wall. Struct.*, **122**, 8-16. https://doi.org/10.1016/j.tws.2017.09.033.
Mohammadimehr, M. and Mehrabi, M. (2017), "Stability and free vibration analyses of double-bonded micro composite sandwich cylindrical shells conveying fluid flow", *Appl. Math. Model.*, **47**, 685-709. https://doi.org/10.1016/j.apm.2017.03.054.
Mohammadimehr, M. and Mostafavifar, M. (2016), "Free vibration analysis of sandwich plate with a transversely flexible core and FG-CNTs reinforced nanocomposite face sheets subjected to magnetic field and temperature-dependent material properties using SGT", *Compos. Part B*, **94**, 253-270. https://doi.org/10.1016/j.compositesb.2016.03.030.
Mohammadimehr, M. and Rahmati, A.H. (2013), "Small scale effect on electro-thermo-mechanical vibration analysis of single-walled boron nitride nanorods under electric excitation", *Turkish J. Eng. Environ. Sci.*, **37**(1), 1-15. DOI:10.3906/muh-1201-17.
Mohammadimehr, M., Mehrabi, M., Hadizadeh, H. and Hadizadeh, H. (2018b), "Surface and size dependent effects on static, buckling, and vibration of micro composite beam under thermo-magnetic fields based on strain gradient theory", *Steel Compos. Struct.*, **26**(4), 513-531. https://doi.org/10.12989/scs.2018.26.4.513.
Mohammadimehr, M., Mohammadi-Dehabadi, A.A., Alavi, S.M.A., Alambeigi, K., Bamdad, M., Yazdani, R. and Hanifehlou, S. (2018c), "Bending, buckling, and free vibration analyses of carbon nanotube reinforced composite beams and experimental tensile test to obtain the mechanical properties of nanocomposite", *Steel Compos. Struct.*, **29**(3), 405-422. https://doi.org/10.12989/scs.2018.29.3.405.
Mohammadimehr, M., Okhravi, S.V. and Akhavan Alavi, S.M. (2018a), "Free vibration analysis of magneto-electro-elastic cylindrical composite panel reinforced by various distributions of CNTs with considering open and closed circuits boundary conditions based on FSDT", *J. Vib. Control*, **24**(8), 1551-1569. https://doi.org/10.1177/1077546316664022.
Mohammadimehr, M., Rostami, R. and Arefi, M. (2016), "Electro-elastic analysis of a sandwich thick plate considering FG core and composite piezoelectric layers on Pasternak foundation using TSDT", *Steel Compos. Struct.*, **20**(3), 513-543. https://doi.org/10.12989/scs.2016.20.3.513.
Mohammadimehr, M., Rousta Navi, B. and Ghorbanpour Arani, A. (2015), "Surface stress effect on the nonlocal biaxial buckling and bending analysis of polymeric piezoelectric nanoplate reinforced by CNT using Eshelby-Mori-Tanaka approach", *J. Solid Mech.*, **7**(2), 173-190.
Mohammadimehr, M., Shahedi, S. and Rousta Navi, B. (2017a), "Nonlinear vibration analysis of FG-CNTRC sandwich Timoshenko beam based on modified couple stress theory subjected to longitudinal magnetic field using generalized differential quadrature method", *Proc. Inst. Mech. Eng., Part C: J. Mech. Eng. Sci.*, **231**(20), 3866-3885. https://doi.org/10.1177/0954406216653622.
Mohammadimehr, M., Zarei, H.B., Parakandeh, A. and Arani, A.G. (2017b), "Vibration analysis of double-bonded sandwich microplates with nanocomposite facesheets reinforced by symmetric and un-symmetric distributions of nanotubes under multi physical fields", *Struct. Eng. Mech.*, **64**(3), 361-379. https://doi.org/10.12989/sem.2017.64.3.361.
Moradi Dastjerdi, R. and Aghadavoudi, F. (2018), "Static analysis of functionally graded nanocomposite sandwich plates reinforced by defected CNT", *Compos. Struct.*, **200**, 839-848. https://doi.org/10.1016/j.compstruct.2018.05.122.
Motezaker, M. and Kolahchi, R. (2017), "Seismic response of SiO2nanoparticles-reinforced concrete pipes based on DQ and newmark methods", *Comput. Concrete*, **19**(6), 745-753. https://doi.org/10.12989/cac.2017.19.6.745.
Nasihatgozar, M., Daghigh, V., Eskandari, M., Nikbin, K. and Simoneau, A. (2016), "Buckling analysis of piezoelectric cylindrical composite panels reinforced with carbon nanotubes", *Int. J. Mech. Sci.*, **107**, 69-79. https://doi.org/10.1016/j.ijmecsci.2016.01.010.
Sodano, H.A., Inman, D.J. and Park, G. (2004), "A review of power harvesting from vibration using piezo-electric materials", *Shock Vib. Dig.*, **36**(3), 197-205.
Studziński, R., Pozorski, Z. and Garstecki, A. (2015), "Structural behavior of sandwich panels with asymmetrical boundary conditions", *J. Constr. Steel Res.*, **104**, 227-234. https://doi.org/10.1016/j.jcsr.2014.10.011.
Tomar, S.S. and Talha, M. (2019), "Influence of material uncertainties on vibration and bending behaviour of skewed sandwich FGM plates", *Compos. Part B: Eng.*, **163**, 779-793. https://doi.org/10.1016/j.compositesb.2019.01.035.
Tornabene, F. (2009), "Free vibration analysis of functionally graded conical, cylindrical shell and annular plate structures with a four-parameter power-law distribution", *Comput. Meth. Appl Mech. Eng.*, **198**(37-40), 2911-2935. https://doi.org/10.1016/j.cma.2009.04.011.
Tornabene, F. and Brischetto, S. (2018), "3D capability of refined GDQ models for the bending analysis of composite and sandwich plates, spherical and doubly-curved shells", *Thin Wall. Struct.*, **129**, 94-124. https://doi.org/10.1016/j.tws.2018.03.021.
Tornabene, F., Fantuzzi, N., Bacciocchi, M. and Viola, E. (2015), "Effect of agglomeration on the natural frequencies of functionally graded carbon nanotube-reinforced laminated composite doubly-curved shells", *Compos. Part B Eng.*, **89**(1), 187-218. https://doi.org/10.1016/j.compositesb.2015.11.016.
Tornabene, F., Fantuzzi, N., Viola, E. and Batra, R.C. (2015), "Stress and strain recovery for functionally graded free-form and doubly-curved sandwich shells using higher-order equivalent single layer theory", *Compos. Struct.*, **119**(1), 67-89. https://doi.org/10.1016/j.compstruct.2014.08.005.
Tornabene, F., Liverani, A. and Caligiana, G. (2011), "FGM and laminated doubly curved shells and panels of revolution with a free-form meridian: A 2-D GDQ solution for free vibrations", *Int. J. Mech. Sci.*, **53**(6), 446-470. https://doi.org/10.1016/j.ijmecsci.2011.03.007.
Trabelsi, S., Frikha, A., Zghal, S. and Dammak, F. (2019), "A

modified FSDT-based four nodes finite shell element for thermal buckling analysis of functionally graded plates and cylindrical shells", *Eng. Struct.*, **178**, 444-459. https://doi.org/10.1016/j.engstruct.2018.10.047.

Xiang, X.M., You, Z. and Lu, G. (2018), "Rectangular sandwich plates with Miura-ori folded core under quasi-static loadings", *Compos. Struct.*, **195**, 359-374. https://doi.org/10.1016/j.compstruct.2018.04.084.

Yuan, S. and Jin, Y. (1998), "Computation of elastic buckling loads of rectangular thin plates using the extended Kantorovich method", *Comput. Struct.*, **66**(6), 861-867. https://doi.org/10.1016/S0045-7949(97)00111-9.

Yun, B.K., Park, Y.K., Lee, M., Lee, N., Jo, W., Lee, S. and Jung, J.H. (2014), "Lead-free $LiNbO_3$ nanowirebased nanocomposite for piezoelectric power generation", *Nanosc. Res. Lett.*, **9**(4), 1-7. https://doi.org/10.1186/1556-276X-9-4.

Zamani, A., Kolahchi, R. and Bidgoli, M.R. (2017), "Seismic response of smart nanocomposite cylindrical shell conveying fluid flow using HDQ-Newmark methods", *Comput. Concrete*, **20**(6), 671-682. https://doi.org/10.12989/cac.2017.20.6.671.

Zghal, S., Frikha, A. and Dammak, F. (2018), "Mechanical buckling analysis of functionally graded power based and carbon nanotubes-reinforced composite plates and curved panels", *Compos. Part B: Eng.*, **150**, 165-183. https://doi.org/10.1016/j.compositesb.2018.05.037.

CC

Appendix A

The values for resultant forces and moments, higher order stresses and electrical displacement are defined as relationships (A.1) to (A.22).

$$M_{xx} = \int_{\frac{hc}{2}}^{\frac{H}{2}} \sigma_{xx} z dz + \int_{\frac{-hc}{2}}^{\frac{hc}{2}} \sigma_{xx} z dz + \int_{\frac{-H}{2}}^{\frac{-hc}{2}} \sigma_{xx} z dz \quad (A.1)$$

$$M_{yy} = \int_{\frac{hc}{2}}^{\frac{H}{2}} \sigma_{yy} z dz + \int_{\frac{-hc}{2}}^{\frac{hc}{2}} \sigma_{yy} z dz + \int_{\frac{-H}{2}}^{\frac{-hc}{2}} \sigma_{yy} z dz \quad (A.2)$$

$$M_{xy} = \int_{\frac{hc}{2}}^{\frac{H}{2}} \tau_{xy} z dz + \int_{\frac{-hc}{2}}^{\frac{hc}{2}} \tau_{xy} z dz + \int_{\frac{-H}{2}}^{\frac{-hc}{2}} \tau_{xy} z dz \quad (A.3)$$

$$P_{1x} = \int_{\frac{hc}{2}}^{\frac{H}{2}} 2Gl_0^2 \gamma_x z \ dz + \int_{\frac{-hc}{2}}^{\frac{hc}{2}} 2Gl_0^2 \gamma_x z \ dz + \int_{\frac{-H}{2}}^{\frac{-hc}{2}} 2Gl_0^2 \gamma_x z \ dz \quad (A.4)$$

$$P_{1y} = \int_{\frac{hc}{2}}^{\frac{H}{2}} 2Gl_0^2 \gamma_y z \ dz + \int_{\frac{-hc}{2}}^{\frac{hc}{2}} 2Gl_0^2 \gamma_y z \ dz + \int_{\frac{-H}{2}}^{\frac{-hc}{2}} 2Gl_0^2 \gamma_y z \ dz \quad (A.5)$$

$$P_{0z} = \int_{\frac{hc}{2}}^{\frac{H}{2}} 2Gl_0^2 \gamma_y dz + \int_{\frac{-hc}{2}}^{\frac{hc}{2}} 2Gl_0^2 \gamma_y dz + \int_{\frac{-H}{2}}^{\frac{-hc}{2}} 2Gl_0^2 \gamma_y dz \quad (A.6)$$

$$T_{1xxx} = \int_{\frac{hc}{2}}^{\frac{H}{2}} 2Gl_1^2 \eta_{xxx} z dz + \int_{\frac{-hc}{2}}^{\frac{hc}{2}} 2Gl_1^2 \eta_{xxx} z dz + \int_{\frac{-H}{2}}^{\frac{-hc}{2}} 2Gl_1^2 \eta_{xxx} z dz \quad (A.7)$$

$$T_{1xxy} = \int_{\frac{hc}{2}}^{\frac{H}{2}} 2Gl_1^2 \eta_{xxy} z dz + \int_{\frac{-hc}{2}}^{\frac{hc}{2}} 2Gl_1^2 \eta_{xxy} z dz + \int_{\frac{-H}{2}}^{\frac{-hc}{2}} 2Gl_1^2 \eta_{xxy} z dz \quad (A.8)$$

$$T_{0xxz} = \int_{\frac{hc}{2}}^{\frac{H}{2}} 2Gl_1^2 \eta_{xxz} dz + \int_{\frac{-hc}{2}}^{\frac{hc}{2}} 2Gl_1^2 \eta_{xxz} dz + \int_{\frac{-H}{2}}^{\frac{-hc}{2}} 2Gl_1^2 \eta_{xxz} dz \quad (A.9)$$

$$T_{0xyz} = \int_{\frac{hc}{2}}^{\frac{H}{2}} 2Gl_1^2 \eta_{xyz} dz + \int_{\frac{-hc}{2}}^{\frac{hc}{2}} 2Gl_1^2 \eta_{xyz} dz + \int_{\frac{-H}{2}}^{\frac{-hc}{2}} 2Gl_1^2 \eta_{xyz} dz \quad (A.10)$$

$$T_{1xyy} = \int_{\frac{hc}{2}}^{\frac{H}{2}} 2Gl_1^2 \eta_{xyy} z dz + \int_{\frac{-hc}{2}}^{\frac{hc}{2}} 2Gl_1^2 \eta_{xyy} z dz + \int_{\frac{-H}{2}}^{\frac{-hc}{2}} 2Gl_1^2 \eta_{xyy} z dz \quad (A.11)$$

$$T_{1xzz} = \int_{\frac{hc}{2}}^{\frac{H}{2}} 2Gl_1^2 \eta_{xzz} z dz + \int_{\frac{-hc}{2}}^{\frac{hc}{2}} 2Gl_1^2 \eta_{xzz} z dz + \int_{\frac{-H}{2}}^{\frac{-hc}{2}} 2Gl_1^2 \eta_{xzz} z dz \quad (A.12)$$

$$T_{1yyy} = \int_{\frac{hc}{2}}^{\frac{H}{2}} 2Gl_1^2 \eta_{yyy} z dz + \int_{\frac{-hc}{2}}^{\frac{hc}{2}} 2Gl_1^2 \eta_{yyy} z dz + \int_{\frac{-H}{2}}^{\frac{-hc}{2}} 2Gl_1^2 \eta_{yyy} z dz \quad (A.13)$$

$$T_{0yyz}=\int_{\frac{hc}{2}}^{\frac{H}{2}}2Gl_1^{\,2}\eta_{yyz}dz+\int_{\frac{-hc}{2}}^{\frac{hc}{2}}2Gl_1^{\,2}\eta_{yyz}dz+\int_{\frac{-H}{2}}^{\frac{-hc}{2}}2Gl_1^{\,2}\eta_{yyz}dz \quad (A.14)$$

$$T_{1yzz}=\int_{\frac{hc}{2}}^{\frac{H}{2}}2Gl_1^{\,2}\eta_{yzz}zdz+\int_{\frac{-hc}{2}}^{\frac{hc}{2}}2Gl_1^{\,2}\eta_{yzz}zdz+\int_{\frac{-H}{2}}^{\frac{-hc}{2}}2Gl_1^{\,2}\eta_{yzz}zdz \quad (A.15)$$

$$T_{0zzz}=\int_{\frac{hc}{2}}^{\frac{H}{2}}2Gl_1^{\,2}\eta_{zzz}dz+\int_{\frac{-hc}{2}}^{\frac{hc}{2}}2Gl_1^{\,2}\eta_{zzz}dz+\int_{\frac{-H}{2}}^{\frac{-hc}{2}}2Gl_1^{\,2}\eta_{zzz}dz \quad (A.16)$$

$$R_{0x}=\int_{\frac{hc}{2}}^{\frac{H}{2}}2Gl_2^{\,2}\chi_{xx}dz+\int_{\frac{-hc}{2}}^{\frac{hc}{2}}2Gl_2^{\,2}\chi_{xx}dz+\int_{\frac{-H}{2}}^{\frac{-hc}{2}}2Gl_2^{\,2}\chi_{xx}dz \quad (A.17)$$

$$R_{0y}=\int_{\frac{hc}{2}}^{\frac{H}{2}}2Gl_2^{\,2}\chi_{yy}dz+\int_{\frac{-hc}{2}}^{\frac{hc}{2}}2Gl_2^{\,2}\chi_{yy}dz+\int_{\frac{-H}{2}}^{\frac{-hc}{2}}2Gl_2^{\,2}\chi_{yy}dz \quad (A.18)$$

$$R_{0yx}=\int_{\frac{hc}{2}}^{\frac{H}{2}}2Gl_2^{\,2}\chi_{xy}dz+\int_{\frac{-hc}{2}}^{\frac{hc}{2}}2Gl_2^{\,2}\chi_{xy}dz+\int_{\frac{-H}{2}}^{\frac{-hc}{2}}2Gl_2^{\,2}\chi_{xy}dz \quad (A.19)$$

$$\begin{aligned}D_{1x}=&\int_{\frac{hc}{2}}^{\frac{H}{2}}\left(\frac{\partial}{\partial x}\psi(x,y,t)\cos(\frac{\pi z}{h})\eta_{11}-e_{11}z\frac{\partial^2}{\partial x^2}w(x,y,t)\right.\\&\left.-e_{12}z\frac{\partial^2}{\partial y^2}w(x,y,t)\right)\cos^2(\frac{\pi z}{h})dz\\&+\int_{\frac{-H}{2}}^{\frac{-hc}{2}}\left(\frac{\partial}{\partial x}\psi(x,y,t)\cos(\frac{\pi z}{h})\eta_{11}-e_{11}z\frac{\partial^2}{\partial x^2}w(x,y,t)\right.\\&\left.-e_{12}z\frac{\partial^2}{\partial y^2}w(x,y,t)\right)\cos^2(\frac{\pi z}{h})dz\end{aligned} \quad (A.20)$$

$$\begin{aligned}D_{1y}=&\int_{\frac{hc}{2}}^{\frac{H}{2}}\left(\eta_{22}\frac{\partial}{\partial y}\psi(x,y,t)\right)\cos^2(\frac{\pi z}{h})dz\\&+\int_{\frac{-H}{2}}^{\frac{-hc}{2}}\left(\eta_{22}\frac{\partial}{\partial y}\psi(x,y,t)\right)\cos^2(\frac{\pi z}{h})dz\end{aligned} \quad (A.21)$$

$$\begin{aligned}D_{1z}=&\int_{\frac{hc}{2}}^{\frac{H}{2}}-h^2\eta_{33}\psi(x,y,t)\sin^2\left(\frac{\pi z}{h}\right)\pi^2dz\\&+\int_{\frac{-H}{2}}^{\frac{-hc}{2}}-h^2\eta_{33}\psi(x,y,t)\sin^2\left(\frac{\pi z}{h}\right)\pi^2dz\end{aligned} \quad (A.22)$$

By placing the Eqs. (A.1) to (A22) in the governing Eq. (27), Eqs. (A.23) and (A.24) are obtained without dependence on each other.

$$\begin{aligned}&1/12C_{12}\left(\frac{\partial^4}{\partial x^2\partial y^2}w(x,y,t)\right)H^3-1/12C_{12}\\&\left(\frac{\partial^4}{\partial x^2\partial y^2}w(x,y,t)\right)h_c^{\,3}+Gl_2^{\,2}H\frac{\partial^4}{\partial x^4}w(x,y,t)\\&+Gl_2^{\,2}H\frac{\partial^4}{\partial y^4}w(x,y,t)-1/15Gl_1^{\,2}H^3\frac{\partial^6}{\partial x^6}w\\&(x,y,t)-1/2Gl_0^{\,2}H^3\frac{\partial^6}{\partial x^4\partial y^2}w(x,y,t)\\&-1/2Gl_0^{\,2}H^3\frac{\partial^6}{\partial x^2\partial y^4}w(x,y,t)-1/6Gl_0^{\,2}H^3\frac{\partial^6}{\partial y^6}w(x,y,t)\\&-1/5G-1/5Gl_1^{\,2}H^3\frac{\partial^6}{\partial x^2\partial y^4}w(x,y,t)\\&-1/15Gl_1^{\,2}H^3\frac{\partial^6}{\partial y^6}w(x,y,t)+\frac{28}{75}Gl_1^{\,2}H\frac{\partial^4}{\partial x^4}w(x,y,t)\\&+\frac{92}{75}Gl_1^{\,2}H\frac{\partial^4}{\partial y^4}w(x,y,t)+2Gl_0^{\,2}H\frac{\partial^4}{\partial x^4}w(x,y,t)\\&+4Gl_0^{\,2}H\frac{\partial^4}{\partial x^2\partial y^2}w(x,y,t)+2Gl_0^{\,2}H\frac{\partial^4}{\partial y^4}w(x,y,t)\\&-1/6Gl_0^{\,2}H^3\frac{\partial^6}{\partial x^6}w(x,y,t)\\&+\frac{8}{15}Gl_1^{\,2}\left(\frac{\partial^4}{\partial x^2\partial y^2}w(x,y,t)\right)H+2Gl_2^{\,2}\left(\frac{\partial^4}{\partial x^2\partial y^2}w(x,y,t)\right)H\\&+1/12C_{11}\left(\frac{\partial^4}{\partial x^4}w(x,y,t)\right)H^3\\&-1/12C_{11}\left(\frac{\partial^4}{\partial x^4}w(x,y,t)\right)h_c^{\,3}+1/12C_{22}\left(\frac{\partial^4}{\partial y^4}w(x,y,t)\right)H^3\\&+1/3C_{66}H^3\frac{\partial^4}{\partial x^2\partial y^2}w(x,y,t)\\&-1/3C_{66}\left(\frac{\partial^4}{\partial x^2\partial y^2}w(x,y,t)\right)h_c^{\,3}\\&+1/3\left(\frac{\partial^4}{\partial x^2\partial y^2}w(x,y,t)\right)Q66h_c^{\,3}\\&+1/12\left(\frac{\partial^4}{\partial x^4}w(x,y,t)\right)Q11h_c^{\,3}\\&1/12\left(\frac{\partial^4}{\partial x^2\partial y^2}w(x,y,t)\right)Q12h_c^{\,3}-1/12C_{22}\left(\frac{\partial^4}{\partial y^4}w(x,y,t)\right)h_c^{\,3}\\&+1/12\left(\frac{\partial^4}{\partial x^2\partial y^2}w(x,y,t)\right)Q_{12}h_c^{\,3}\\&+1/12\left(\frac{\partial^4}{\partial y^4}w(x,y,t)\right)Q_{22}h_c^{\,3}-K_g\frac{\partial^2}{\partial x^2}w(x,y,t)\\&-K_g\frac{\partial^2}{\partial y^2}w(x,y,t)+K_ww(x,y,t)\\&-q(x,y)-1/12C_{21}\left(\frac{\partial^4}{\partial x^2\partial y^2}w(x,y,t)\right)h_c^{\,3}\\&+1/12C_{21}\left(\frac{\partial^4}{\partial x^2\partial y^2}w(x,y,t)\right)H^3\end{aligned} \quad (A.23)$$

$$
-1/6\left(\begin{array}{l}
-4\left(\frac{\partial^2}{\partial x^2}\psi(x,y,t)\right)\left(\cos\left(1/2\frac{\pi H}{h}\right)\right)^2\sin\left(1/2\frac{\pi H}{h}\right)\eta_{11}h^3\\
+4\left(\frac{\partial^2}{\partial x^2}\psi(x,y,t)\right)\left(\cos\left(1/2\frac{\pi h_c}{h}\right)\right)^2\sin\left(1/2\frac{\pi h_c}{h}\right)\eta_{11}h^3\\
-6\psi(x,y,t)\pi^2\cos\left(1/2\frac{\pi H}{h}\right)\sin\left(1/2\frac{\pi H}{h}\right)\eta_{33}h+\\
6\psi(x,y,t)\pi^2\cos\left(1/2\frac{\pi h_c}{h}\right)\sin\left(1/2\frac{\pi h_c}{h}\right)\eta_{33}h\\
-6\left(\frac{\partial^2}{\partial y^2}\psi(x,y,t)\right)\cos\left(1/2\frac{\pi H}{h}\right)\sin\left(1/2\frac{\pi H}{h}\right)\eta_{22}h^3\\
+6\left(\frac{\partial^2}{\partial y^2}\psi(x,y,t)\right)\cos\left(1/2\frac{\pi h_c}{h}\right)\sin\left(1/2\frac{\pi h_c}{h}\right)\eta_{22}h^3+3H\psi(x,y,t)\pi^3\eta_{33}\\
-3H\left(\frac{\partial^2}{\partial y^2}\psi(x,y,t)\right)\pi\eta_{22}h^2-3\psi(x,y,t)\pi^3\eta_{33}h_c\\
-8\left(\frac{\partial^2}{\partial x^2}\psi(x,y,t)\right)\sin\left(1/2\frac{\pi H}{h}\right)\eta_{11}h^3+8\left(\frac{\partial^2}{\partial x^2}\psi(x,y,t)\right)\sin\left(1/2\frac{\pi h_c}{h}\right)\eta_{11}h^3\\
+3\left(\frac{\partial^2}{\partial y^2}\psi(x,y,t)\right)\pi\eta_{22}h^2h_c
\end{array}\right)h^{-2}\pi^{-1}
\tag{A.24}
$$

$$
\begin{aligned}
&-1/5Gl_1^2H^3\left(\frac{d^4}{dx^4}f(x)\right)\frac{d^2}{dy^2}g(y)-1/15Gl_1^2H^3f(x)\frac{d^6}{dy^6}g(y)+2Gl_0^2Hf(x)\frac{d^4}{dy^4}g(y)\\
&+4Gl_0^2H\left(\frac{d^2}{dx^2}f(x)\right)\frac{d^2}{dy^2}g(y)+Gl_2^2Hf(x)\frac{d^4}{dy^4}g(y)+K_wf(x)g(y)+1/12C_{11}\left(\frac{d^4}{dx^4}f(x)\right)g(y)H^3\\
&-1/12C_{12}\left(\frac{d^2}{dx^2}f(x)\right)\left(\frac{d^2}{dy^2}g(y)\right)h_c^3+1/12C_{12}\left(\frac{d^2}{dx^2}f(x)\right)\left(\frac{d^2}{dy^2}g(y)\right)H^3-1/12C_{21}\left(\frac{d^2}{dx^2}f(x)\right)\left(\frac{d^2}{dy^2}g(y)\right)h_c^3\\
&+1/12\left(\frac{d^2}{dx^2}f(x)\right)\left(\frac{d^2}{dy^2}g(y)\right)Q_{12}h_c^3+1/3C_{66}H^3\left(\frac{d^2}{dx^2}f(x)\right)\frac{d^2}{dy^2}g(y)\\
&+1/12f(x)\left(\frac{d^4}{dy^4}g(y)\right)Q_{22}h_c^3-1/12C_{22}f(x)\left(\frac{d^4}{dy^4}g(y)\right)h_c^3+1/12C_{21}\left(\frac{d^2}{dx^2}f(x)\right)\left(\frac{d^2}{dy^2}g(y)\right)H^3\\
&+1/12C_{22}f(x)\left(\frac{d^4}{dy^4}g(y)\right)H^3-1/12C_{11}\left(\frac{d^4}{dx^4}f(x)\right)g(y)h_c^3-1/3C_{66}\left(\frac{d^2}{dx^2}f(x)\right)\left(\frac{d^2}{dy^2}g(y)\right)h_c^3\\
&-K_g\left(\frac{d^2}{dx^2}f(x)\right)g(y)-K_gf(x)\frac{d^2}{dy^2}g(y)+1/3\left(\frac{d^2}{dx^2}f(x)\right)\left(\frac{d^2}{dy^2}g(y)\right)Q_{66}h_c^3+1/12\left(\frac{d^2}{dx^2}f(x)\right)\left(\frac{d^2}{dy^2}g(y)\right)Q_{21}h_c^3\\
&-1/15Gl_1^2H^3\left(\frac{d^6}{dx^6}f(x)\right)g(y)+2Gl_2^2\left(\frac{d^2}{dx^2}f(x)\right)\left(\frac{d^2}{dy^2}g(y)\right)H-1/5Gl_1^2H^3\left(\frac{d^2}{dx^2}f(x)\right)\frac{d^4}{dy^4}g(y)\\
&-1/2Gl_0^2H^3\left(\frac{d^4}{dx^4}f(x)\right)\frac{d^2}{dy^2}g(y)-1/2Gl_0^2H^3\left(\frac{d^2}{dx^2}f(x)\right)\frac{d^4}{dy^4}g(y)-1/6Gl_0^2H^3f(x)\frac{d^6}{dy^6}g(y)\\
&-1/6Gl_0^2H^3\left(\frac{d^6}{dx^6}f(x)\right)g(y)+Gl_2^2H\left(\frac{d^4}{dx^4}f(x)\right)g(y)+\frac{8}{15}Gl_1^2\left(\frac{d^2}{dx^2}f(x)\right)\left(\frac{d^2}{dy^2}g(y)\right)H\\
&\frac{92}{75}Gl_1^2Hf(x)\frac{d^4}{dy^4}g(y)+2Gl_0^2H\left(\frac{d^4}{dx^4}f(x)\right)g(y)+\frac{28}{75}Gl_1^2H\left(\frac{d^4}{dx^4}f(x)\right)g(y)-q(x,y)\\
&+1/12\left(\frac{d^4}{dx^4}f(x)\right)g(y)Q_{11}h_c^3
\end{aligned}
\tag{A.25}
$$

$$
\left\{\begin{array}{l}
m_0'=g(Y)\quad m_1'=\frac{d}{dY}g(Y)\quad m_2'=\frac{d^2}{dY^2}g(Y)\ m_3'=\frac{d^3}{dY^3}g(Y)\\
m_6'=\frac{d^6}{dY^6}g(Y)\ m_4'=\frac{d^4}{dY^4}g(Y)\quad m_5'=\frac{d^5}{dY^5}g(Y)
\end{array}\right.
\tag{A.26}
$$

$$\dddot{A}_0 = \frac{1}{36\cos(\varphi)^4} 36m_0K_w\cos(\varphi)^4 + 3m_4C_{22}H^3 - 3m_4C_{22}hc^3 + 72m_4Gl_0^2H + 46m_4Gl_1^2H$$
$$+36m_4Gl_2^2H + 3m_4Q_{22}hc^3 - 36K_gm_2\cos(\varphi)^2 \tag{A.27}$$

$$\dddot{A}_1 = -\frac{1}{45}\tan(\varphi)15m_3\cos(\varphi)^2C_{22}H^3 - 15m_3\cos(\varphi)^2C_{22}hc^3 - 45m_5Gl_0^2H^3 - 18m_5Gl_1^2H^3$$
$$+360m_3\cos(\varphi)^2Gl_0^2H + 230m_3\cos(\varphi)^2Gl_1^2H + 180m_3\cos(\varphi)^2Gl_2^2H + 15m_3\cos(\varphi)^2Q_{22}hc^3$$
$$-90K_gm_1\cos(\varphi)^4 \tag{A.28}$$

$$\dddot{A}_2 = \frac{1}{60\cos(\varphi)^6}(360m_2\cos(\varphi)^2Gl_2^2H + 460m_2\cos(\varphi)^2Gl_1^2H + 720m_2\cos(\varphi)^2Gl_0^2H - 360m_2\cos(\varphi)^6Gl_2^2H$$
$$-428m_2\cos(\varphi)^4Gl_1^2H - 480m_2\cos(\varphi)^4Gl_0^2H + 120m_4\cos(\varphi)^2Gl_0^2H^3 + 48m_4\cos(\varphi)^2Gl_1^2H^3 - 60K_gm_0\cos(\varphi)^4$$
$$-150Gl_0^2H^3m_4 - 60Gl_1^2H^3m_4 + 30m_2\cos(\varphi)^2C_{22}H^3 - 30m_2\cos(\varphi)^2C_{22}h_c^3 + 30m_2\cos(\varphi)^2Q_{22}h_c^3 - 30m_2\cos(\varphi)^4C_{22}H^3$$
$$+30m_2\cos(\varphi)^4C_{22}h_c^3 - 30m_2\cos(\varphi)^4Q_{22}h_c^3 - 20m_2\cos(\varphi)^4C_{66}h_c^3 + 20m_2\cos(\varphi)^4Q_{66}h_c^3 + 5m_2\cos(\varphi)^4C_{12}H^3$$
$$-5m_2\cos(\varphi)^4C_{12}h_c^3 + 5m_2\cos(\varphi)^4Q_{12}h_c^3 + 5m_2\cos(\varphi)^4C_{21}H^3 - 5m_2\cos(\varphi)^4C_{21}h_c^3 + 5m_2\cos(\varphi)^4Q_{21}h_c^3 + 20m_2\cos(\varphi)^4C_{66}H^3) \tag{A.29}$$

$$\dddot{A}_3 = \frac{-1\sin(\varphi)}{90\cos(\varphi)^6}(120m_3\cos(\varphi)^2Gl_0^2H^3 + 48m_3\cos(\varphi)^2Gl_1^2H^3 + 360m_1\cos(\varphi)^2Gl_2^2H + 460m_1\cos(\varphi)^2Gl_1^2H$$
$$-300m_3Gl_0^2H^3 - 120m_3Gl_1^2H^3 + 30m_1\cos(\varphi)^2C_{22}H^3 - 30m_1\cos(\varphi)^2C_{22}h_c^3 + 30m_1\cos(\varphi)^2Q_{22}h_c^3 - 30m_1\cos(\varphi)^4C_{22}H^3$$
$$+30m_1\cos(\varphi)^4C_{22}h_c^3 - 30m_1\cos(\varphi)^4Q_{22}h_c^3 - 60m_1\cos(\varphi)^4C_{66}h_c^3 + 60m_1\cos(\varphi)^4Q_{66}h_c^3 + 15m_1\cos(\varphi)^4C_{12}H^3$$
$$-15m_1\cos(\varphi)^4C_{12}h_c^3 + 15m_1\cos(\varphi)^4Q_{12}h_c^3 + 15m_1\cos(\varphi)^4C_{21}H^3 - 15m_1\cos(\varphi)^4C_{21}h_c^3 + 15m_1\cos(\varphi)^4Q21h_c^3$$
$$+60m_1\cos(\varphi)^4{}_{C66}H^3 + 720m_1\cos(\varphi)^2Gl_0^2H - 360m_1\cos(\varphi)^4Gl_2^2H - 364m_1\cos(\varphi)^4Gl_1^2H) \tag{A.30}$$

$$\dddot{A}_4 = \frac{1}{900\cos(\varphi)^6}(-2250GH^3l_0^2m_2 - 900GH^3l_1^2m_2 + 1800m_2\cos(\varphi)^2Gl_0^2H^3 + 720m_2\cos(\varphi)^2Gl_1^2H^3 - 1800m_0\cos(\varphi)^4Gl_2^2H$$
$$-1820m_0\cos(\varphi)^4Gl_1^2H + 1006m_0\cos(\varphi)^6Gl_1^2H + 900m_0\cos(\varphi)^2Gl_2^2H + 1150m_0\cos(\varphi)^2Gl_1^2H + 1800m_0\cos(\varphi)^2Gl_0^2H$$
$$+1800m_0\cos(\varphi)^6Gl_2^2H - 150m_0\cos(\varphi)^4C_{22}H^3 + 150m_0\cos(\varphi)^4C_{22}h_c^3 - 150m_0\cos(\varphi)^4Q_{22}h_c^3 + 300m_0\cos(\varphi)^6C_{66}h_c^3$$
$$-300m_0\cos(\varphi)^6Q_{66}h_c^3 - 75m_0\cos(\varphi)^6C_{12}H^3 + 75m_0\cos(\varphi)^6C_{12}h_c^3 - 75m_0\cos(\varphi)^6Q_{12}h_c^3 - 75m_0\cos(\varphi)^6C_{21}H^3$$
$$+75m_0\cos(\varphi)^6C_{21}h_c^3 - 75m_0\cos(\varphi)^6Q_{21}h_c^3 - 300m_0\cos(\varphi)^6C_{66}H^3 + 75m_0\cos(\varphi)^2C_{22}H^3 - 75m_0\cos(\varphi)^2C_{22}h_c^3$$
$$+75m_0\cos(\varphi)^2Q_{22}h_c^3 - 300m_0\cos(\varphi)^4C_{66}h_c^3 + 300m_0\cos(\varphi)^4Q_{66}h_c^3 + 75m_0\cos(\varphi)^4C_{12}H^3 - 75m_0\cos(\varphi)^4C_{12}h_c^3$$
$$+75m_0\cos(\varphi)^4Q_{12}h_c^3 + 75m_0\cos(\varphi)^4C_{21}H^3 - 75m_0\cos(\varphi)^4C_{21}h_c^3 + 75m_0\cos(\varphi)^4Q_{21}h_c^3 + 300m_0\cos(\varphi)^4C_{66}H^3$$
$$+75m_0\cos(\varphi)^6C_{11}H^3 - 7m_0\cos(\varphi)^6C_{11}h_c^3 + 75m_0\cos(\varphi)^6Q_{11}h_c^3 + 75m_0\cos(\varphi)^6C_{22}H^3 - 75m_0\cos(\varphi)^6C_{22}h_c^3$$
$$+75m_0\cos(\varphi)^6Q_{22}h_c^3) \tag{A.31}$$

$$\dddot{A}_5 = \frac{1}{5}\frac{m_1\sin(\varphi)GH^3\left(5l_0^2 + 2l_1^2\right)}{\cos(\varphi)^6} \tag{A.32}$$

$$\dddot{A}_6 = -\frac{1}{30}\frac{GH^3\left(5l_0^2 + 2l_1^2\right)m_0}{\cos(\varphi)^6} \tag{A.33}$$